Reviewed Preprint
v1 • July 14, 2025
Not revised

Reviewed Preprint
v2 • April 24, 2026
Revised by authors

Unreliable homeostatic action potential broadening in cultured dissociated neurons

Andreas Ritzau-Jost[1], Salil Rajayer[2,3], Jana Nerlich[1], Filip Maciag[4], Alexandra John[1], Michael Russier[5], Victoria Gonzalez Sabater[6,7], Luke J Steiger[2,3], Jacques-Olivier Coq[5], Jens Eilers[1], Maren Engelhardt[8,9,10], Juan Burrone[6,7], Dominique Debanne[5], Martin Heine[4], Stephen M Smith[2,3], Stefan Hallermann[1]

[1]Carl-Ludwig-Institute of Physiology, Faculty of Medicine, Leipzig University, Leipzig, Germany • [2]Division of Pulmonary and Critical Care Medicine, Department of Medicine, Oregon Health and Science University, Portland, United States • [3]Section of Pulmonary and Critical Care Medicine, VA Portland Health Care System, Portland, United States • [4]Institute for Developmental Biology and Neurobiology, Johannes Gutenberg University, Mainz, Germany • [5]Unité de Neurobiologie des canaux Ioniques et de la Synapse (UNIS), UMR_S 1072, INSERM, Aix-Marseille Université, Marseille, France • [6]MRC Centre for Neurodevelopmental Disorders, Institute of Psychiatry, Psychology and Neuroscience, King's College London, London, United Kingdom • [7]Centre for Developmental Neurobiology, Institute of Psychiatry, Psychology and Neuroscience, King's College London, London, United Kingdom • [8]Institute of Neuroanatomy, Mannheim Center for Translational Neuroscience, Medical Faculty Mannheim, Heidelberg University, Mannheim, Germany • [9]Institute of Anatomy and Cell Biology, Johannes Kepler University, Linz, Austria • [10]Clinical Research Institute for Neurosciences, Johannes Kepler University, Linz, Austria

For correspondence:
andreas.ritzau.jost@gmail.com
smisteph@ohsu.edu
hallermann@medizin.uni-leipzig.de

Competing interests: No competing interests declared

Funding: See page 20

Reviewing editor: Teresa Giraldez, Universidad de La Laguna, Spain

eLife Assessment

This study provides **compelling** evidence that action potential (AP) broadening is not a universal feature of homeostatic plasticity in response to chronic activity deprivation. By leveraging state-of-the-art methods across multiple brain regions and laboratories, the authors demonstrate that AP half-width remains largely stable, challenging previous assumptions in the field. These **important** findings help resolve longstanding inconsistencies in the literature and significantly advance our understanding of neuronal network homeostasis. The authors have clarified methodological differences with prior work and expanded the discussion of potential mechanisms, strengthening the interpretation of the findings without altering the central conclusions.

https://doi.org/10.7554/eLife.106995.2.sa4

Abstract

Homeostatic plasticity preserves neuronal activity against perturbations. Recently, somatic action potential broadening was proposed as a key homeostatic adaptation to chronic inactivity in neocortical neurons. Since action potential shape critically controls calcium entry and neuronal function, broadening provides an attractive homeostatic feedback mechanism to regulate activity. Here, we report that chronic inactivity induced by sodium channel block does not broaden action potentials in neocortical neurons under a wide range of conditions. In contrast, action potentials were broadened in CA3 neurons of organotypic hippocampal cultures by chronic sodium channel block and in hippocampal dissociated cultures by chronic synaptic block. Mechanistically, BK-type potassium channels were proposed to underly inactivity-induced action potential broadening. However, BK channels did not affect action potential duration in our recordings. Our results indicate that action potential broadening can occur in specific neurons and conditions but is not a general mechanism of homeostatic plasticity in cultured neurons.

Introduction

Action potentials (APs) control various functions including neurotransmitter release from axonal boutons[1], calcium signals in the soma[2], and synaptic plasticity in dendrites[3]. AP broadening during short-term plasticity on the time scale of milliseconds to seconds is well-established and occurs in many types of neuronal cell bodies[4,5] and nerve terminals[6,7]. There are also indications that APs change during long-term plasticity on the time scale of minutes to hours. When examining Hebbian long-term plasticity (i.e., positive feedback-based and input-specific long-term plasticity[8]), some studies reported AP broadening. For example, presynaptic APs of hippocampal mossy fiber boutons broaden during depolarization-induced potentiation[9] and somatic APs of neurons in the amygdala broaden during fear conditioning[10]. In contrast, the role of the AP duration is less clear for non-Hebbian homeostatic long-term plasticity (i.e., negative feedback-based and non-input specific long-term plasticity[8]). Specifically, homeostatic plasticity induced by neuronal inactivity in the presence of the sodium channel blocker tetrodotoxin (TTX) has been studied for decades, but AP broadening was initially not described[11,12]. A recent study however reports prominent AP broadening during TTX-induced homeostatic plasticity at the soma of cultured neocortical neurons[13], which was not observed at presynaptic boutons of cultured neocortical neurons[14]. Compartmentalized AP broadening at the neuronal cell body would provide a strikingly simple and previously overlooked mechanism by which neuronal inactivity could increase subsequent excitability[13]. This mechanism involves decreased calcium entry during TTX application causing changes in gene expression that would result in broadened APs and more calcium entry after TTX removal. In this model, AP broadening is a key link in the homeostatic feedback loop underlying homeostatic plasticity. In a collaborative effort across several laboratories, we therefore systematically investigated AP broadening in cultured neurons during homeostatic plasticity under various experimental conditions.

Results

Cell type- and model-specific AP broadening in hippocampal neurons

APs in CA3 neurons of hippocampal organotypic slice cultures broaden homeostatically upon chronic inactivity using both, synaptic block by glutamate receptor antagonists[15] or sodium channel block by TTX[16] (see also ref. 17 for a similar trend). We first aimed to confirm homeostatic AP broadening in CA3 neurons in organotypic slice cultures. APs were elicited by depolarizing currents from the resting membrane potential during perfusion with TTX-free artificial cerebrospinal fluid. APs recorded in CA3 pyramidal neurons treated with TTX (48 hours) had longer durations than those in control cells (Fig. 1A, B; median [IQR] 1.75 [1.69–1.86] ms and 2.13 [2.07–2.22] ms for control and TTX-treatment, respectively, 14 cells each, $P < 0.001$), confirming earlier reports of homeostatic AP broadening in these neurons[15,16].

Next, we tested whether homeostatic AP broadening occurred in dissociated hippocampal cultured neurons, a model widely used to study homeostatic plasticity. We inhibited neuronal activity for 48 hours to induce homeostatic plasticity by either blocking AP firing using TTX (Fig. 1C) or by blocking synaptic transmission using the low-affinity glutamate receptor blocker kynurenic acid (Kyn) or the high-affinity glutamate receptor blocker 2,3-Dioxo-6-nitro-1,2,3,4-tetrahydrobenzo [f]quinoxaline-7-sulfonamide (NBQX). Surprisingly, AP duration was unaffected by TTX-treatment in primary hippocampal cultured neurons (Fig. 1D; median [IQR] 2.07 [1.79–2.34] ms and 2.08 [1.32–2.61] ms for control and TTX, 25 and 24 cells, respectively, $P = 0.96$). In contrast, Kyn-treatment significantly increased AP duration in the same set of interleaved experiments (Fig. 1D; median [IQR] 2.52 [2.31–2.72] ms, 22 cells, $P = 0.014$) and NBQX-treatment led to a small trend towards broader APs (Fig. 1D; $P = 0.26$). Importantly, sodium channel block and synaptic block both increased spontaneous AP firing frequency, indicating that homeostatic adaptations other than AP broadening were shared between both induction methods (Fig. 1E, F; $P = 0.008$ for control against Kyn, $P = 0.005$ for control against NBQX, $P = 0.013$ for control against

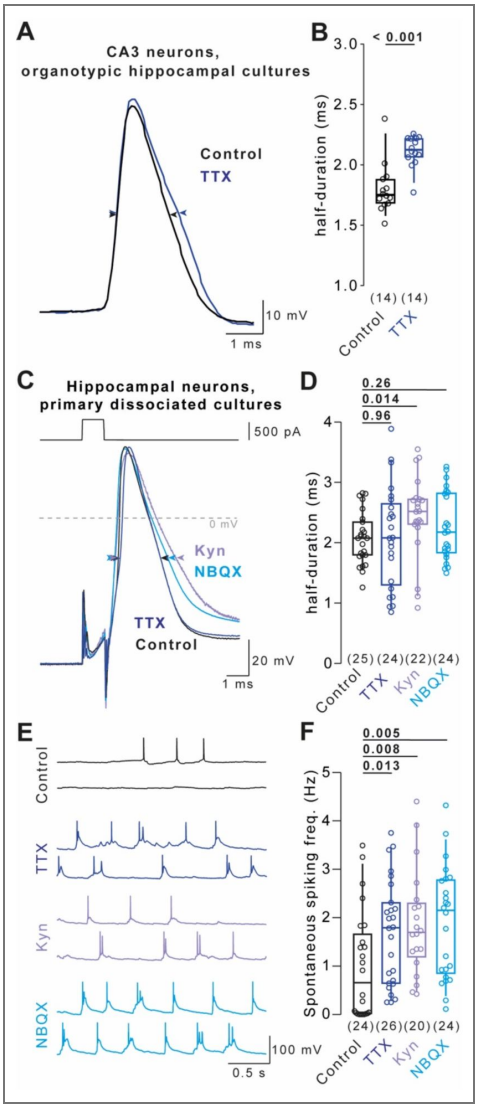

Figure 1. Cell type- and model-specific AP broadening in hippocampal neurons

(A) Example evoked APs recorded from CA3 pyramidal neurons in organotypic hippocampal cultures under control condition (black) and following 48 hours of TTX-treatment (blue). (B) AP durations recorded under conditions in A. (C) Example depolarization-evoked APs (500 pA for 1 ms) recorded from neurons in primary dissociated hippocampal cultures under control condition (black) and following 48 hours of TTX- (blue), Kyn- (purple), or NBQX-treatment (turquoise). (D) AP durations recorded under conditions in C. (E) Example spontaneous APs recorded under the conditions in C. (F) Spontaneous AP frequency under the conditions in C. Numbers in brackets reflect number of recorded neurons. Box plots as median ± interquartile range, whiskers indicate 10–90 percentile. P-values above graphs, significance tested by Mann-Whitney-*U* test.

TTX). These data indicate that AP broadening occurred upon sodium channel block in CA3 neurons in organotypic slice cultures and upon synaptic block in dissociated hippocampal cultures, but not in the commonly-studied model of homeostatic plasticity using dissociated hippocampal cultured neurons and 48 hours of TTX application.

Stable AP duration in primary dissociated neurons during TTX-induced homeostatic plasticity

In contrast to our finding in dissociated cultured neurons of the hippocampus, a recent study described TTX-induced AP broadening in dissociated cultured neurons of the neocortex[13]. To resolve this discrepancy, we set out to replicate AP broadening in neocortical cultured neurons. Given that exact reproduction of experimental conditions is challenging and neuronal plasticity depends on brain region[18], animal species[19], and animal strain[20], we probed homeostatic AP broadening under different experimental conditions varying: 1) experimental animal species (rat and mouse), 2) strain (C57BL/6 and CD1 mice), 3) sub-strain (C57BL/6N and C57BL/6J mice), 4) brain area (cortex and hippocampus), 5) cortical subdomain (prefrontal cortex), 6) culture duration (10–14, 15–21, and 32 days *in vitro*), 7) culture growth medium, 8) recording solutions, and 9) laboratory and experimenter performing recordings (conditions I–X in Fig. 2B, condition XI are recordings from Fig. 1; see also Fig. 2 – figure supplement 1). Even though AP durations varied up to 2-fold between conditions, statistically significant homeostatic AP broadening was not detectable in any of the tested conditions (Fig. 2B). To minimize type II errors (false negative) we intentionally did not apply a correction for multiple comparisons. The only significance was observed in condition III but in an opposite direction (i.e. AP narrowing with TTX, P=0.026; Fig. 2B). However, this is likely a false positive because application of corrections for false discovery rate results in P=0.268 for both Benjamini–Hochberg and Bonferroni correction. To detect cross-conditional AP broadening by TTX, we merged all conditions based on their difference in AP duration after TTX-treatment (Fig. 2C). However, AP duration was the same in control and TTX-treated cells (217 and 197 cells, respectively, P = 0.83).

We next tested whether AP broadening was concealed by systematic differences in neuronal health or recording quality between control and treatment group. Because unhealthy neurons tend to have small and slow APs, possibly due to changes in resting membrane potential or expression of voltage-gated sodium and potassium channels, we first analyzed AP amplitude as a measure of neuronal viability. AP amplitudes were not affected following TTX treatment in any of the eleven recording conditions (Fig. 2D) or a cross-conditional comparison (Fig. 2E). In addition, we focused on the culture protocol or cortical subdomain previously associated with AP broadening[13] (conditions I, VII, and VIII) and applied further inclusion criteria to rigorously discriminate healthy excitatory neurons: the occurrence of multiple APs upon 200 ms-current injections (≥ 2 APs), a resting membrane potential below – 55 mV, and a maximum AP depolarization rate between 100 and 337 V/s (includes 96% of excitatory and exclude >80% of the inhibitory neurons; ref. 21). Applying any or all three of these criteria did not reveal AP broadening upon TTX treatment (Fig. 2 – figure supplement 2). These data indicate that stricter exclusion criteria result in smaller variability in action potential duration but do not uncover AP broadening in these datasets.

Instead of depolarization-evoked APs, Li *et al.*[13] recorded hyperpolarization-evoked 'rebound APs' (Fig. 2F), possibly reducing the impact of different resting membrane potentials and depolarizing current injection on the AP waveform. We determined that the duration of rebound APs was similarly unaffected by TTX treatment across all recorded conditions (Fig. 2G, H). These data show that TTX-induced AP broadening does not robustly occur in dissociated cultured neurons.

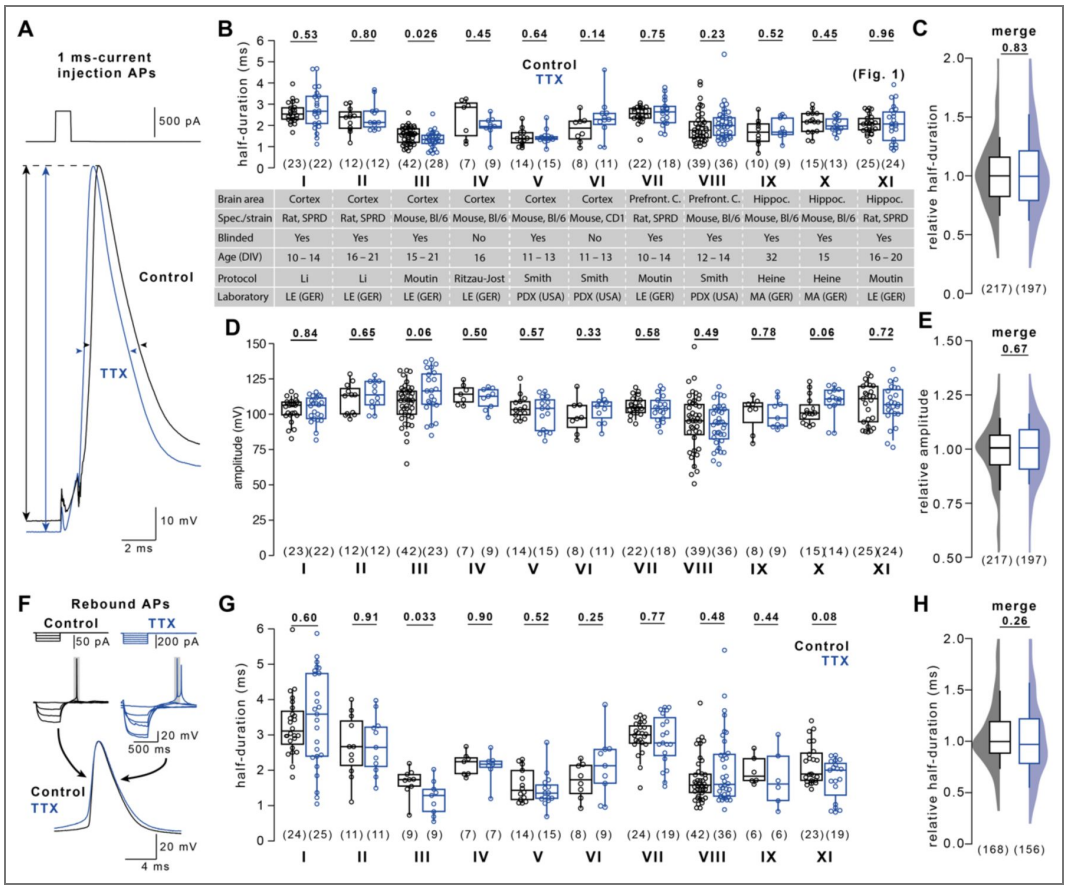

Figure 2. Stable AP duration in primary dissociated neurons during TTX-induced homeostatic plasticity

(A) Example current injection-evoked APs (500 pA for 1 ms) under control condition (black) and following 48 hours of TTX-treatment (blue). AP amplitudes are recorded between the membrane potential preceding the AP and AP peak (arrows), AP durations are recorded at half-maximal amplitude (arrow heads). (B) AP duration in control and TTX-treated cells (color code as in A) for eleven different experimental conditions (I–XI). Specification of individual conditions is provided in Table S1. Condition XI adopted from Fig. 1D. (C) Merge of AP durations in control and TTX-treated cells across conditions I–IX normalized to the corresponding condition's control median duration. (D) AP amplitudes in control and TTX-treated cells as in B. (E) Cross-conditional merge of AP amplitudes in control and TTX-treated cells as in C. (F) Example hyperpolarization-evoked "rebound APs" (-150 pA or -60 pA for 500ms) in control and TTX-treated cells (color code as in A). (G) Rebound AP duration in control and TTX-treated cells as in B. (H) Cross-conditional merge of normalized durations as in C for rebound APs. Numbers in brackets reflect number of recorded neurons. Box plots as median ± interquartile range, whiskers indicate 10–90 percentile. P-values provided above graphs; significance tested using Mann-Whitney-*U* tests.

Homeostatic plasticity increases network activity and excitatory synaptic transmission

To verify successful induction of homeostatic plasticity under our experimental conditions, we quantified changes in neuronal activity and synaptic strength following TTX-induced homeostatic plasticity. TTX-treatment increased the number of spontaneously active neurons (Fig. 3A; merge of conditions I–IV and VII; control: 23 out of 87 cells, TTX-treatment: 58 out of 74 cells, $P < 0.001$ with Fisher's exact test) and the number of APs per spontaneous burst (Fig. 3B, C; median [IQR] 1.0 [1.0–1.12] APs and 1.67 [1.0–2.71] APs for control and for TTX-treatment, 23 and 58 cells, respectively, $P < 0.001$). These results indicate an adaptive increase in neuronal activity following TTX-treatment, in line with previous findings on homeostatic plasticity[16,22,23]. Furthermore, spontaneous excitatory postsynaptic currents (sEPSCs; spontaneous synaptic currents recorded in the absence of TTX) were recorded as a measure of synaptic strength (Fig. 3D). sEPSC frequency and amplitude increased upon TTX-treatment (Fig. 2E, merge of recordings from condition I and II; median [IQR] frequency 1.11 [0.42–1.47] Hz and 5.07 [1.95–5.52] Hz in control and TTX-treated cells, 16 and 11, respectively, $P = 0.027$; median [IQR] amplitude 12.4 [10.6–14.4] pA and 15.5 [14.1–17.4] pA in control and TTX-treated cells, 16 and 11 cells, respectively, $P = 0.042$), in accord with known homeostatic synaptic adaptations to inactivity[24–27]. These changes in sEPSC amplitude and frequency are not specific for somatic, pre-or postsynaptic adaptations. However, the results show that blocking AP firing with TTX successfully induced homeostatic plasticity under our experimental conditions.

Lack of BK channel-dependent AP broadening in dissociated cultured neurons

Various potassium channel subtypes regulate AP repolarization and could therefore underlie AP broadening. Li *et al.*[13] reported that downregulation of BK-type potassium channels led to homeostatic AP broadening in neocortical cultured neurons. We tested the role of BK channels in AP repolarization (neurons grown under condition I). However, blocking BK channels with Iberiotoxin (IbTx, 300 nM) did not lead to broadening of depolarization-evoked APs in control and TTX-treated cells (Fig. 4A; $P = 0.10$ and 0.48, respectively), or a merge of both conditions (Fig. 4B; $P = 0.10$). Rebound APs were similarly unaffected by BK channel block (Fig. 4 – figure supplement 1). Next, we tested whether recurrent neuronal activity, which increases cytosolic calcium and boosts BK-channel activity, enhanced AP broadening following TTX treatment. While APs significantly broadened during repetitive firing, AP durations were similar in control and TTX-treated neurons (Fig. 4C and D), suggesting no differential regulation of BK-channels following TTX-treatment in these recordings.

In electrical recordings, intracellular recording solution may have disturbed cytosolic calcium dynamics and therefore BK- and thus calcium-dependent AP repolarization. As an independent approach, we recorded the AP duration in hippocampal cultured neurons using the genetically encoded voltage indicator (GEVI) Ace-mNeon[28] before and after acute IbTx perfusion (100 nM). BK channel block did not affect AP duration in the soma or along the axon (Fig. 4E). Using the GEVI, we again tested the role of BK channels in AP broadening during a train of APs (5 APs at 20 Hz, Fig. 4F). The broadening of somatic, proximal axonal, and distal axonal APs during trains was similar before and after BK channel block, indicating that AP duration was not modulated by BK channels. To confirm that IbTx was indeed pharmacologically active in Ace-mNeon recordings, we preconditioned cells with 4-AP (30 µM) prior to IbTx perfusion (Fig. 4G). Neurons preconditioned with 4-AP had broader somatic APs which were further broadened by IbTx, presumably due to increased calcium influx following 4-AP treatment, in turn activating more BK channels[29]. These data indicate that IbTx application was pharmacologically active but BK channels did not contribute to AP repolarization in cultured neocortical neurons.

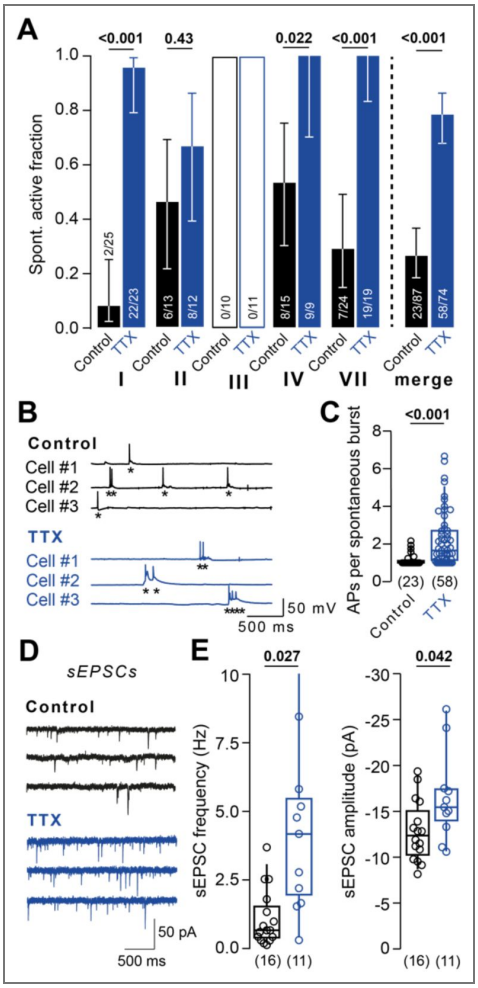

Figure 3. Homeostatic plasticity increases network activity and excitatory synaptic transmission

(A) *Left:* Spontaneously active control (black) and TTX-treated cells (blue) in condition I–IV and VII. *Right*: Active neurons merged across conditions I–IV and VII. (B) Example spontaneous AP bursts in control and TTX-treated cells. Asterisks mark individual APs. (C) AP number per burst in control and TTX-treated cells across conditions I–IV and VII. (D) Example spontaneous excitatory postsynaptic currents (sEPSCs) in control and TTX-treated cells. (E) *Left:* sEPSC frequency and *Right:* sEPSC amplitude in control recordings and after TTX-treatment (merged data from conditions I and II). Numbers in brackets reflect number of recorded neurons. Bars in A reflect fraction of spontaneously active neurons. Whiskers in A reflect confidence limits for 95% confidence interval based on Wilson interval. Box plots as median ± interquartile range, whiskers indicate 10–90 percentile. P-values above graphs, significance tested by Fisher's exact test in A or Mann-Whitney-*U* test elsewhere.

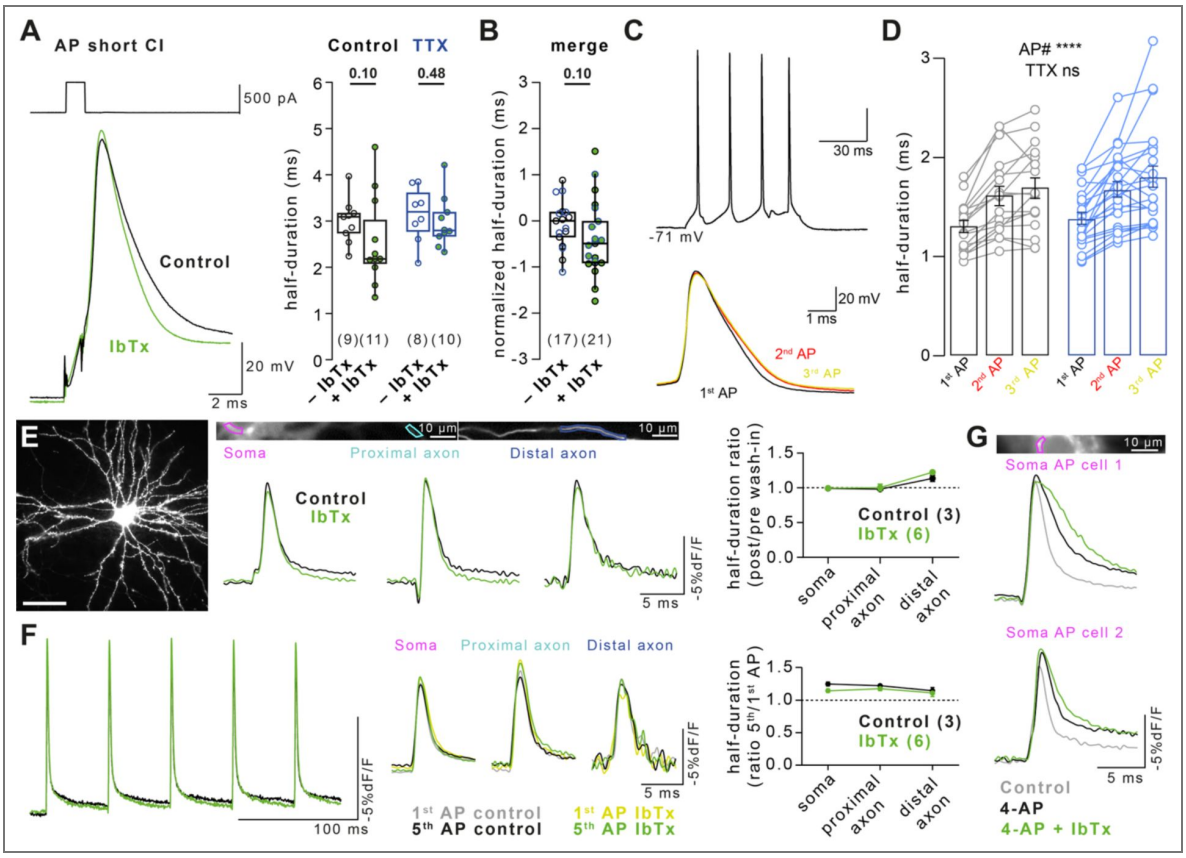

Figure 4. Lack of BK channel-dependent AP broadening in dissociated cultured neurons

(A) *Left:* Example current injection-evoked APs (500 pA for 1 ms) in control solution (black) and solution containing 300 nM Iberiotoxin (IbTx, green). *Right:* AP duration in control and TTX-treated cells recorded IbTx-free (black and blue, respectively) or IbTx-containing solution (green). Data recorded under condition I. (B) Merged AP duration across control and TTX-treated cells for recordings in IbTx-free and IbTx-containing solution (data in A normalized to the respective group's median duration in control solution). (C) APs evoked by a 200 ms current injection (top) and overlay of the forst three evoked APs (bottom).(D) Broadening of AP duration of the 3 first APs during 200 ms current injections in control (black, *left*) and TTX-treated cells (blue, *right*). Bars as mean ± SEM, lines with markers depict recordings from individual neurons. (E) *Left:* Example image of neuron expressing the genetically encoded voltage indicator Ace-mNeon (scale bar 50 µm). *Middle:* Example Ace-mNeon-recorded somatic, proximal axonal, and distal axonal APs in a primary hippocampal cultured neuron in IbTx-free solution (black) and following BK channel block by IbTx (100 nM, green). *Right:* Ratio of somatic and axonal AP durations in IbTx-free and IbTx-containing solution. (F) *Left:* Example AP train (5 x 20 Hz) and overlay of 1st and 5th train AP at the soma, proximal, and distal axon in control condition (grey and black) and following BK channel block by IbTx (yellow and green). *Right:* AP broadening (ratio of 5th over 1st train AP duration) in the three compartments in control and IbTx-containing solution. (G) Somatic APs under control condition (grey), following treatment with 4-AP (black), and following treatment with 30µM 4-AP + 100 nM IbTx (green). Numbers in brackets reflect number of recorded neurons. Box plots as median ± interquartile range, whiskers indicate 10–90 percentile. Plots in D–F as mean ± SEM. P-values above graphs, significance tested by Mann-Whitney-*U* test.

Discussion

Homeostatic AP broadening has been reported in some systems, but it has not been tested systematically across experimental models so far. Because BK channels that were proposed to underlie AP broadening are activated by depolarization and calcium[30,32], we studied APs elicited with depolarizations from the RMP where BK activity was presumably increased, as well as anode break ('rebound') APs thought to obviate variance from ion channel inactivation. We found that broadening of rebound and depolarization-evoked APs did not occur following the induction of homeostatic plasticity with TTX in the most commonly studied model system (primary dissociated neuronal cultures). However, AP broadening was observed in cultured hippocampal slices. Furthermore, blocking BK channels, which were reported to mediate AP broadening during homeostatic plasticity[13], did not impact AP duration in dissociated cultured neurons. Our results therefore indicate that AP broadening in cultured dissociated neurons is not a required component of homeostatic plasticity.

TTX-induced homeostatic AP regulation in organotypic hippocampal cultured neurons

AP broadening was previously shown to occur in CA3 neurons of organotypic hippocampal slice cultures following TTX-induced homeostatic plasticity[16]. Consistently, we recorded broader APs in CA3 neurons following neuronal inactivity (Fig. 1). In contrast to CA3 neurons, granule cells of the dentate gyrus did not show TTX-induced AP broadening[17]. Similarly, CA1 neurons did not show AP broadening following synaptic block-induced homeostatic plasticity[31]. Therefore, we conclude that homeostatic AP broadening in organotypic hippocampal cultures is most likely cell type-specific.

TTX-induced homeostatic AP regulation in primary dissociated cultured neurons

To the best of our knowledge, only three studies so far reported on the duration of APs following TTX-induced homeostatic plasticity in dissociated cultured neurons[13,33,34]. While Li *et al.*[13] observed TTX-induced broadening, the studies by Lee, Chung, and others[33,34] reported stable AP duration, consistent with our findings (Fig. 2). Furthermore, in other studies investigating TTX-induced homeostatic plasticity in dissociated cultured neurons, prominent AP broadening was either missed or absent (see for example refs. 23,35–37). One possible explanation for this inconsistency could be the cell type-specificity of AP broadening. We focused on large, presumably excitatory neurons. However, we and others could have selected different neuron types compared to Li *et al.*[13]. In an attempt to reduce bias, we incorporated multi-lab, randomization, and blinding strategies across many of our experiments. Only recordings with leaky seal formation or inadequate capacitance compensation[38] were excluded. However, in a subset of experimental conditions we applied additional exclusion criteria to ensure that variability in neuron type, health or recording quality were not causing a type II (false negative) statistical error. Application of these exclusion criteria did not reveal AP broadening in our data (Fig. 2 – figure supplement 2), confirming that AP broadening was not associated with homeostatic plasticity in neocortical neurons following TTX treatment.

The sensitivity to chronic TTX treatment might depend on baseline neuronal activity, which is in part related to neuronal culture density[39]. However, TTX did not induce AP broadening despite different baseline activities (Fig. 3A) and a nearly threefold variation in the number of plated cells per cover slip between conditions (25k – 70k cells per cover slip). Although we mainly focus on neocortical cultured neurons (condition I to VIII, Fig. 2) because Li *et al.* used neocortical neurons, the absence of AP broadening in hippocampal neurons (group IX to XI) could in principle be explained by the selective loss of CA3 neurons, which show AP broadening in organotypic cultured neurons (Fig. 1A and B). However, CA3 neurons were shown to survive in dissociated cultures following region-specific microdissection[40], and CA1 neurons are generally more stress-sensitive to excitotoxicity with glutamate or NMDA than CA3 and DG neurons[42],

arguing against a general selective loss of CA3 neuron in dissociated cultures. Altered cell-cell interactions with glia and neurons in organotypic and dissociated neuronal cultures could instead contribute to the different findings in various hippocampal preparations.

Synaptic block-induced homeostatic AP regulation in primary dissociated cultured neurons

Homeostatic AP broadening was shown in CA3 neurons upon activity block by the low-affinity glutamate receptor blocker Kyn[15]. We similarly observed Kyn-induced AP broadening in dissociated cultured hippocampal neurons (Fig. 1C, D). In contrast, APs were not significantly broader following synaptic block by NBQX (Fig. 1C, D), in accord with recordings from CA1 neurons in organotypic cultures using CNQX. TTX-induced broadening may therefore be cell-type specific or due to a differential effect of the glutamate receptor blockers on NMDA receptors which are blocked by Kyn but not NBQX/CNQX or TTX and which have recently been demonstrated to be important for the induction of synaptic homeostatic plasticity[41]. Further studies are needed to investigate the role of subcellular calcium signals in the regulation of AP duration in hippocampal neurons during block of glutamate receptors.

Absence of BK channel-dependent AP broadening in dissociated cultured neurons

Li *et al.*[13] proposed that BK channels hasten AP repolarization and that this effect is lost during TTX-induced homeostatic plasticity, leading to AP broadening. We did not detect AP broadening when blocking BK channels in either control or TTX-treated cells (Fig. 4). Furthermore, because calcium accumulation following multiple APs has been shown to enhance intraspike BK contribution in some neurons[43] we compared how 1st, 2nd, or 3rd APs were impacted by prior TTX-exposure. AP broadening did occur in the later APs but the changes were unaffected by TTX exposure (Fig. 4D), suggesting no activity-dependent effect of TTX or BK channels on AP duration.

Voltage imaging using Ace-mNeon similarly showed that duration of single APs and broadening during AP trains in the soma and axon were unaffected by BK channel block. Blocking BK channels only affected AP repolarization when cells were preconditioned with 4-AP. These results are consistent with previous reports showing that in some neurons BK channels do not contribute to repolarization[43,44] while doing so in others[44–47]. Differences in the abundance of other types of potassium channels[44] and intracellular calcium buffering[46] are known to affect the contribution of BK channels to AP repolarization and may account for the lack of AP broadening upon BK channel block in our dissociated cultured neurons. Alternatively, BK activity may occur only under conditions associated with elevated intracellular[30,32]. The lack of BK channel contribution to AP repolarization in our dissociated neurons is another possible explanation (in addition to different selection of cells) for why we and others have not observed the homeostatic AP broadening described by Li *et al.*[13].

Inactivity-induced homeostatic AP regulation *in vivo*

Homeostatic plasticity has also been studied using *in vivo* recordings from the activity-suppressed visual cortex[48,49]. The majority of these studies reported stable AP duration upon monocular deprivation or chemogenetic activity suppression[50–52]. In contrast, Li *et al.*[13] found homeostatically broadened APs in the visual cortex upon monocular deprivation. Furthermore, stable AP duration was also observed in other brain areas following activity suppression such as (1.) the somatosensory cortex upon unilateral whisker trimming[53–58] or forepaw denervation[59], (2.) the auditory system upon cochlear ablation[60,61], hearing loss[62], or congenital deafness[63], (3.) the vestibular nucleus upon vestibular ablation[64], and (4.) the olfactory mitral cells upon naris occlusion[65] or senescent hippocampal deafferentiation[66]. Besides somatic APs, APs in excitatory

presynaptic terminals of the somatosensory thalamus were also unaffected by whisker deprivation[67]. Thus, AP broadening does not appear to occur robustly upon suppression of neuronal activity in various neuronal pathways.

Hyperactivity-induced homeostatic AP regulation

Homeostatic plasticity occurs not only upon activity block but also upon hyperactivity, generally involving opposite adaptations. In cultured neurons, AP duration was unaffected following hyperactivity induced by chronic depolarization[68], block of potassium channels[69], block of inhibitory synaptic transmission[31,33,34], or chronic ChR2-induced photostimulation[70]. In contrast, Li *et al.*[13] reported similar BK channel downregulation upon both, TTX-induced activity block and depolarization-induced hyperactivity.

As in cultured neurons, AP duration was mostly unaffected in brain slice recordings from animals with increased neuronal activity due to an enriched environment[58,71,72], psychosocial stress[73], or febrile seizures[74]. AP shortening occurred in cerebellar granule cells after exposure to an enriched environment[75], in auditory neurons following chronic noise exposure[76], and in hippocampal neurons following age-related[77] or pilocarpine-induced hyperactivity[78]. Thus, in contrast to Li *et al.*[13], AP duration was either unaffected or, if anything, shortened during hyperactivity-induced homeostatic plasticity in previous studies.

In this study, several laboratories collaborated to determine the robustness of inactivity-induced AP broadening. AP broadening did not occur upon TTX-treatment in dissociated hippocampal or neocortical neurons. Furthermore, BK channel block did not affect AP duration in dissociated neurons, arguing against BK channels as mediators of a general homeostatic AP regulation.

Despite the lack of homeostatic, TTX-induced AP broadening in dissociated cultures, AP duration was broadened upon Kyn-treatment in dissociated cultures and using TTX in CA3 neurons in organotypic cultures. Because BK-channels control AP duration in CA3 neurons of organotypic cultures[79], homeostatic BK-channel downregulation as proposed by Li *et al.* may be involved in AP broadening in this specific cell type. While the reasons for the variable occurrence of homeostatic AP broadening remain unknown, this may render neuronal circuitries more robust to perturbations. The regulation of AP duration therefore might represent one element in the repertoire of neuronal plasticity that is, similar to other plasticity mechanisms, not generally shared, but specifically expressed in some cell types and neuronal compartments.

Methods

Ethics

At all times animal procedures were in accordance with the relevant international, national and institutional guidelines for the care and use of laboratory animals (European Council Directive 86/609/EEC, U.S. Public Health Service Policy on Humane Care and Use of Laboratory Animals, U.S. National Institutes of Health Guide for the Care and Use of Laboratory Animals, German Tierschutzgesetz, French National Research Council guidelines, and Leipzig and Mainz University guidelines). All animal procedures were approved in advance by the local health authorities (Ethics Committees at Leipzig University and Mainz University, federal Saxonian Animal Welfare Committee, the District administration Mainz-Bingen (41a/177-5865-§11 ZVTE), the Committee of the Préfecture des Bouches-du-Rhône (D13055-08), V.A. Portland Health Care System Institutional Animal Care and Use Committee).

Animal models

Organotypic hippocampal cultures were generated from postnatal day 5–7 Wistar rats. Dissociated neocortical cultures were generated from postnatal day 0 or 1 Sprague-Dawley rats (conditions I, II and VII), C57BL/6N mice (conditions III and IV), C57BL/6J mice (conditions V and VIII), or CD1 mice (condition VI). Dissociated hippocampal cultures were generated from postnatal day 0 or 1 C57BL/6N mice (conditions IX), C57BL/6J mice (condition X), or Sprague-Dawley rats (condition XI).

Generally, animals of both sexes were used to generate cultures. Mother animals were kept in individually ventilated cages under a 12h/12h light-dark cycle and received water and food *ad libitum*.

Induction of Homeostatic Plasticity

Homeostatic plasticity was induced by inclusion of one of the respective blockers in culture medium for 48–56 hours prior to recordings. All blockers were first diluted in 100 µL of fresh medium per treated well and subsequently added to the respective wells containing 1 mL of medium. For control conditions, only 100 µL of fresh medium without blockers was added to the respective wells. The blockers had final concentrations of (in mM): 0.002 tetrodotoxin (TTX; Tocris, Wiesbaden-Nordenstadt, Germany), 2 kynurenic acid (Kyn), or 0.01 2,3-Dioxo-6-nitro-1,2,3,4-tetrahydrobenzo-[f]quinoxaline-7-sulfonamide (NBQX). To avoid bias, coverslips were randomized to treatment (control or blocker) and recordings were made and analyzed in a blinded fashion (except for condition IV and VI). Blinding was performed by an independent investigator. Control or TTX-treatment groups were assigned using an 8-block randomization approach for experiments of condition VIII. Unblinding of the experimental groups was performed after analysis and disclosure of the data by the experimenter.

Preparation of dissociated neocortical cultures

Conditions I and II (Hallermann Lab, Leipzig, Germany)

Neocortical cultures were generated as described by Li *et al.*[13]. Shortly, neocortices were isolated and dissected into 5–10 pieces per hemisphere. Samples were washed twice in ice-cold modified HBSS (4.2 mM $NaHCO_3$ and 1 mM HEPES, pH 7.35, 300 mOsm) supplemented with 20% fetal bovine serum (FBS) and digested at 37 °C for 30 min using papain. After stopping digestion with 20% FBS-containing modified HBSS, samples were washed and dissociated using Pasteur pipettes, pelleted twice, and filtered using a 70 nm nylon strainer. 30.000–50.000 vital dissociated cells were plated on poly-D-lysine-coated 14 mm coverslips and cultured in NbActive4 medium (Transnetyx, Cordova, TN, USA) in an incubator until use (37 °C, 5% CO_2 in room air, water vapor saturated).

Conditions III and VII (Hallermann Lab, Leipzig, Germany)

Cultures were generated as previously described by Moutin *et al.*[80]. In brief, mice were decapitated and neocortices (for condition III) or the frontal third of neocortices (for condition VII) were isolated in ice-cold Hibernate-A medium (Thermo Fisher Scientific, Waltham, MA, USA) and cut into 5–10 chunks. Chunks were first digested by papain (dissolved in Hibernate-A; 10 min at 37 °C) and subsequently by papain + DNAse (125 µL of 20 mg/mL DNAse stock; 5 min at 37 °C). Digestion was stopped by CM+ medium (Neurobasal A 86.5 %, B27 2 %, Glutamax 0.25 %, L-Glutamine 0.25%, penicillin G/streptomycin 1 %, heat-inactivated FBS 10 %) and chunks were mechanically dissociated in two steps by 1250 µL pipette tips with gravity decantation and collection of the supernatant between dissociation steps and after dissociation. Supernatant was passed through 2 mL of frothed bovine serum albumin, centrifuged (7 min, 300 x g), the resulting pellet was resuspended in 1–2 mL of CM+ medium and 25.000–30.000 resuspended vital cells were plated onto poly-L-lysine-coated coverslips. After 30 min, 0.5 mL of CM+ medium was added to the wells and after 2 days *in vitro* (DIV), cytosine arabinoside (ARA-C, 1 µM final concentration) was added to the wells for 8–18 h. Subsequently, 0.4 mL medium per well was replaced by fresh CM- medium (BrainPhys 96.75% by Stemcell Technologies, Vancouver, Canada, B27 2%, Glutamax 0.25%, penicillin G/streptomycin 1%) and further 0.1 mL of medium were exchanged every 6–7 days with fresh CM- medium until cells were used.

Condition IV (Hallermann Lab, Leipzig, Germany)

Cultures were generated following the protocol by Ritzau-Jost *et al.*[14]. In short, mice were decapitated and cerebral cortices were removed, dissected in ice-cold Hank's balanced saline solution, and cut into 5–10 pieces per hemisphere. Samples were digested by Trypsin (5 mg, dissolved in digestion solution; for composition see below) for 5 minutes at 37 °C. Trypsin was stopped by ice-cold MEM growth medium (composition see below), supernatant was discarded,

and samples were mechanically and enzymatically dissociated using Pasteur pipettes of narrowing tip diameters in DNAse-supplemented MEM growth medium (10 mg/mL). The supernatant was centrifuged and the resulting pellet was resuspended in MEM growth medium for plating onto Matrigel-coated 14 mm coverslips (50.000 vital cells/coverslip). Forty-eight hours after plating, the medium was fully replaced by MEM growth medium containing 4 µM ARA-C to limit glial growth. After another 48 hours, the medium was fully replaced by MEM growth medium. Cells were incubated at 37 °C, 93% humidity, and room air plus 5% CO_2 until use. Digestion solution contained the following (in mM): 137 NaCl, 5 KCl, 7 Na_2HPO_4, 25 HEPES, pH adjusted to 7.2 by NaOH. MEM growth medium was prepared from 1l MEM (Earle's salts + L-Glutamine) supplemented with 5 g Glucose, 0.2 g $NaHCO_3$, 0.1 g bovine holo-Transferrin, 0.025 g bovine insulin, 50 mL FBS and 10 mL B-27.

Conditions V, VI and VIII (Smith Lab, Portland, OR, USA)

Cultures were generated following the protocol by Martiszus *et al.*[81]. Briefly, 1–2-day old mice were decapitated following general anesthesia with isoflurane, and their cerebral cortices (for conditions V and VI) or the frontal third of neocortices (for condition VIII) were dissected out while bathed in ice-cold modified Hank's balanced saline solution (modified HBSS; Hyclone laboratories, Logan, UT, USA) and cut into 5–10 pieces per hemisphere. Samples were digested by Trypsin (10 mg, dissolved in digestion solution as mentioned in Condition IV) for 5 minutes at 37 °C. Trypsin was de-activated by ice-cold HBSS with 20% FBS, supernatant was discarded, and samples were enzymatically and mechanically dissociated using Pasteur pipettes with narrowing tip diameters in DNAse-supplemented HBSS. The supernatant was centrifuged and the resulting pellet was resuspended in 5% MEM growth medium (see composition above in Condition IV) for plating 65.000 vital cells onto Matrigel-coated 12 mm glass coverslips. MEM growth medium containing 4 µM ARA-C was added 48 hours later to limit glial proliferation, and subsequently replaced with MEM growth medium following another 48 hours. Cells were incubated at 37 °C, 93% humidity, and room air plus 5% CO_2 until use between days 11–14 *in vitro*.

Preparation of dissociated hippocampal cultures

Condition IX and X (Heine Lab, Mainz, Germany)

In short, mice pups were decapitated and brains were removed. Hippocampi were dissected in ice-cold Hank's balanced saline solution and digested by trypsin for 15 minutes at 37 °C. Next, the tissue was washed with cold HBSS and mechanically dissociated using Pasteur pipettes in DNAse-, glutamate- and FBS-supplemented DMEM growth medium. 100 µL of cell suspension containing approximately 70.000 cells was placed on a glass coverslip and incubated at 37 °C, 5% CO_2 for 1 hour. Coverslips were then transferred to 12-well plates with glutamate-, B27- and sodium pyruvate-supplemented Neurobasal A medium (1 mL per well) and cultivated until use. Double distilled water was added in between the wells of the 12-well plate to prevent evaporation of the medium during cultivation.

Condition XI (Hallermann Lab, Leipzig, Germany)

Cultures were generated as described for Condition III, except that hippocampi from postnatal day 0–1 Sprague-Dawley rats were used for preparation. 25.000–30.000 vital cells were plated per coverslip.

Recordings from dissociated cultures

Within conditions, recordings were performed blinded (except conditions IV and VI) and interleaved from randomized sister coverslips of the same culture, at the same recording setup, and by the same experimenter.

Conditions I – IV, VII and XI (Hallermann Lab, Leipzig, Germany)

Voltage- and current-clamp recordings were performed with borosilicate pipettes using a HEKA EPC10/2 amplifier (HEKA Elektronik, Lambrecht/Pfalz, Germany). Borosilicate glass tubes (Science Products, Hofheim, Germany) were pulled by a DMZ Universal Electrode Puller with filament

heating (Zeitz Instruments, Martinsried, Germany) to 3–6.5 MΩ pipette resistance. Pipettes were filled with internal solution (see *Solutions and reagents* section) and mounted on a micromanipulator (Kleindiek Nanotechnik, Reutlingen, Germany) using a custom-built pipette holder. Recordings were performed at room temperature (22–25 °C). All current-clamp recordings were filtered with the internal 10 kHz 8-pole Bessel filter of the HEKA EPC10/2 amplifier and subsequently digitized (200 kHz) with the HEKA EPC10/2 using Patchmaster software (HEKA Elektronik, Lambrecht/Pfalz, Germany). Built-in compensation was used for voltage offset and pipette capacitance. Membrane potentials were not corrected for liquid junction potential and bridge compensation was adjusted to minimize the current injection artifact. APs were evoked by brief 1 ms depolarizing current injections of 500–1500 pA or 500 ms hyperpolarizing pulses (300–1000 pA) leading to APs upon return to resting membrane potential ('rebound APs'). Both, depolarization-evoked and rebound APs were first recorded at resting membrane potential without holding current. While depolarization readily evoked APs in all conditions, rebound AP did not occur in all conditions at their resting membrane potential. In these cells, holding currents were used to depolarize cells until rebound APs were observed upon long hyperpolarizing pulses. Spontaneous excitatory postsynaptic currents were recorded in voltage-clamp mode at -70 mV membrane potential in neurons grown in conditions I and II. Currents were filtered with the internal 3 kHz 8-pole Bessel filter of the HEKA EPC10/2 amplifier, digitized (200 kHz) and detected using the template matching algorithm [82] implemented in NeuroMatic (Version 2.00, 15.09.2008; ref. [83]).

Conditions V, VI and VIII (Smith Lab, Portland, OR, USA)

Current-clamp recordings were performed with borosilicate pipettes using a HEKA EPC10 amplifier (HEKA Elektronik, Lambrecht/Pfalz, Germany). Patch pipettes (5–10 MΩ resistance) were pulled from thin-walled borosilicate glass tubes (Warner Instruments, Holliston, MA, USA) using a P-87 electrode puller (Sutter Instruments, Novato, CA, USA). Pipettes were filled with an internal solution (see *Solutions and reagents* section) and mounted on a micromanipulator (ROE-200, Sutter Instruments, Novato, CA, USA). Recordings were performed at room temperature (22–25 °C). Voltage signals were filtered at 2.9 kHz and digitized at 20 kHz. Membrane potentials were corrected for liquid junction potential and bridge balance was performed manually prior to data acquisition. All APs were evoked by a sequence of transient injections relative to the resting membrane potential and measurements taken from the APs elicited with the minimal stimulus using either depolarizing current injections (500–1000 pA in 100 pA increments for 1–3 ms in 0.5 ms increments in conditions V and VI or 20–140 pA in 20 pA increments for 0.5 s in condition VIII) or following rebound from longer hyperpolarizing pulses (300–1200 pA in 100 pA increments for 500 ms).

Conditions IX & X (Heine Lab, Mainz, Germany)

Voltage- and current-clamp recordings were performed with borosilicate pipettes using a HEKA EPC9 amplifier (HEKA Elektronik, Lambrecht/Pfalz, Germany). Filamented glass tubes (Science Products, Hofheim, Germany) were pulled by a Narishige PC-100 electrode puller. Resistance of the pipettes was 2–6 MΩ. Pipettes were filled with internal solution (see *Solutions and reagents* section) and mounted on a micromanipulator (Luigs & Neumann, Ratingen, Germany). Recordings were performed at room temperature (21–24 °C). Signals were filtered at 2.9 kHz and digitized at 20 kHz using Patchmaster software (HEKA Elektronik, Lambrecht/Pfalz, Germany). Built-in compensation was used for voltage offset and pipette capacitance. Membrane potentials were not corrected for liquid junction potential. APs were evoked by brief 1 ms depolarizing current injection of 50–300 pA or 500 ms hyperpolarizing pulses (300–400 pA) leading to APs upon return to resting membrane potential ('rebound APs').

Preparation of organotypic hippocampal cultures

Cultures were prepared as described previously[84]. In brief, young Wistar rats (P5–P7) were anesthetized with isoflurane and killed by decapitation, the brain was removed, and each hippocampus was dissected. Hippocampal slices (350 µm) were obtained using a Vibratome (Leica,

VT1200S, Wetzlar, Germany). They were placed on 20 mm latex membranes (Millicell; Merck, Darmstadt, Germany) inserted into 35 mm Petri dishes containing 1 mL of culture medium and maintained for up to 8 days in an incubator at 34 °C, 95% O_2, 5% CO_2. The culture medium contained 25 mL MEM, 12.5 mL HBSS, 12.5 mL horse serum, 0.5 mL penicillin/streptomycin, 0.8 mL glucose (1 M), 0.1 mL ascorbic acid (1 mg/mL), 0.4 mL HEPES (1 M), 0.5 mL B27, and 8.95 mL sterile H_2O. To limit glial proliferation, 5 µM ARA-C was added to the culture medium starting at DIV 4.

AP recordings from organotypic hippocampal cultures

Whole-cell recordings were obtained from CA3 neurons in organotypic cultures at DIV 7 to DIV 10. All recordings were made at 34 °C in a temperature-controlled recording chamber (Luigs & Neumann, Ratingen, Germany) using 7–10 MΩ patch pipettes. CA3 pyramidal neurons were recorded in current-clamp with a Multiclamp 700B Amplifier (Molecular Devices, San Jose, CA, USA). APs were elicited by delivering DC step pulses (duration 1.0 s) at an interstimulus interval of 10–15 s. During the whole recording, ionotropic glutamate and $GABA_A$ receptors were blocked with 2–4 mM kynurenic acid and 100 µM picrotoxin, respectively.

Analysis of APs

Data were analyzed using IGOR PRO software (WaveMetrics, Lake Oswego, OR, USA; Version 6.32A or 6.37), the Patcher's Power Tool (Version 2.19 Carbon, 15.03.2011) and NeuroMatic (Version 2.00, 15.09.2008; ref. [83]) extensions, as well as self-written IGOR PRO scripts. AP durations were quantified as the duration at half-maximal AP amplitude, amplitude being the difference between AP peak and the membrane potential preceding stimulation. When AP durations were recorded at half-maximal amplitude between AP threshold (defined as the membrane potential at which the voltage rate of change first reaches 10 V/s) and AP peak, AP durations were still unaffected by TTX treatment (data not shown). To exclude the effect of mis-balanced bridge compensation on AP shape, only APs that occurred after the end of the second current injection artifact (elicited by the end of current-injection) were analyzed. In some recordings, current injection artifacts were blanked over 50 µs at the beginning and the end of the current injection and only experiments in which blanking did not affect AP amplitude and duration were subsequently analyzed.

Hippocampal dissociated cultures and transfection for GEVI imaging

Culture preparation and GEVI transfection were performed as previously described by Sabater *et al.*[28]. In short, hippocampi were dissected from embryonic day 17.5 Wistar rat pups of either sex, treated with trypsin (Worthington Biochemical Corporation, Lakewood, NJ, USA) at 0.5 mg/mL, and mechanically dissociated using fire polished Pasteur pipettes. Neurons were plated on 18 mm glass coverslips pre-treated with 100 µg/mL poly-L-lysine and coated with 10 µg/mL laminin (Thermo Fisher Scientific, Waltham, MA, USA). Cultures were maintained in Neurobasal medium with B27 (1x) and GlutaMAX (1x, all obtained from Thermo Fisher Scientific, Waltham, MA, USA), supplemented with FBS (2%, Biosera, Nuaille, France) and Penicillin/Streptomycin (1%, Sigma-Aldrich, St. Louis, MO, USA), at 37°C in a humidified incubator with 5% CO_2. For transfections with Ace2N-mNeon-4AA (Ace-mNeon, ref. [85]; distributed by Biolife Solutions Inc., Bothell, WA, USA), the Effectene transfection reagent (Qiagen, Venlo, Netherlands) was used. The medium was changed at DIV 3 to culture medium without antibiotic or FBS, and transfections with Effectene were performed at DIV 7 following the manufacturer's protocol. After transfection neurons were maintained in serum-free media without antibiotics. For all experiments 30% of the medium was changed weekly and neurons were imaged 7–14 days after transfection (14–21 DIV).

GEVI Imaging conditions

GEVI imaging was performed as previously described by Sabater *et al.*[28]. In short, neurons were imaged using an inverted Olympus IX71 epifluorescence microscope with a 60x 1.42 NA oil-immersion objective (Olympus, Tokyo, Japan). Coverslips were mounted in a heated chamber (Warner instruments, Holliston, MA, USA; total volume ~500 µL) and placed on an IMTP

microscope stage (Scientifica, Uckfield, United Kingdom). Cells were maintained in external HEPES-buffered saline solution (HBS: 2 mM $CaCl_2$, 1.6 mM $MgCl_2$, 1.45 mM NaCl, 2.5 mM KCl, 10 mM Glucose, 10 mM HEPES, pH 7.4, Osmolarity 290 mOsm) and experiments were carried out at near physiological temperatures of 32–35 °C.

In Ace-mNeon imaging experiments, ~505 nm excitation illumination was provided using a 525 nm LED (Solis LED, Thorlabs, Newton, NJ, USA), a 500/20 nm excitation filter, and a 510 nm long-pass dichroic mirror. Ace-mNeon emission transmitted through the dichroic was filtered using a 520 nm long-pass filters (Chroma, Bellows Falls, VT, USA). A power density of 10 mW/mm^2 was obtained at the specimen plane. Images were acquired at 3.2 kHz with an ORCA-Flash4.0 V2 C11440-22CU scientific CMOS camera (Hamamatsu Photonics, Hamamatsu, Japan) cooled to ~ -20 °C with the Exos2 water cooling system (Koolance, Auburn, WA, USA). Images were acquired with HCImage software (Hamamatsu, Hamamatsu, Japan), binned to 4 × 4 and cropped to a 16 × 512-pixel region of interest, necessary to achieve the high image acquisition rates. Images were saved in CXD format.

Stimulation of APs was achieved with an extracellular tungsten parallel bipolar electrode (FHC, Bowdoin, ME, USA) mounted on a PatchStar motorized micro-manipulator (Scientifica, Uckfield, United Kingdom). To reliably induce an AP, we delivered a 1 ms 10 mV pulse at the soma. The timing of the LED illumination, the acquisition and stimulation were triggered externally through Clampex software (pClamp 10, Molecular Devices, San Jose, CA, USA).

All GEVI Imaging recordings were performed in presence of NBQX (10 µM), Gabazine (10 µM) and D-2-amino-5-phosphonovalerate (APV, 25 µM; all from Bio-Techne, Wiesbaden-Nordenstadt, Germany) in order to block synaptic transmission and ensure that the observed events were due to the stimulation only. IbTx was delivered using a custom gravity-fed perfusion system and bath volume was maintained by a peristaltic pump (Watson-Marlow 120s; Watson-Marlow, Rommerskirchen, Germany).

Image analysis

Image analysis was performed as previously described by Sabater *et al.*[28]. In short, voltage imaging recordings were analyzed in ImageJ and custom scripts within MATLAB software as follows. Prior to analysis, if drift had occurred in the x and y axis during the recording, the images were aligned using the TurboReg ImageJ plugin[86]. Images were then imported into MATLAB and fluorescence intensity profiles were obtained from regions of interest (ROIs) manually drawn around neuronal structures identified visually on a maximum projection image of the time series by averaging across the ROI pixels in each frame. The fluorescence profile was separated into single trials and corrected for background camera noise by subtracting the average intensity value of the timepoints where no illumination light was applied. Then, recordings were reconstructed at a sampling rate of 100 kHz using cubic spline interpolation. Bleaching was estimated by fitting a single exponential function to each individual trace smoothed using an averaging filter with a window of 3 and interpolated. The resulting curve was used to correct an unfiltered interpolated version of the recording. An accurate representation of the AP waveform with an enhanced SNR was obtained by averaging over the repeats and extracting the AP parameters from the resulting trace. The fluorescence profile during the 20 ms preceding a response was used as baseline.

Solutions and reagents

Reagents were purchased from Sigma-Aldrich (St. Louis, MO, USA) if not indicated otherwise.

Conditions I, II, VII and XI

The extracellular bath solution contained (in mM): 122 NaCl, 3 KCl, 10 D-Glucose, 26 $NaHCO_3$, 1.25 Na_2HPO_4, 1.3 $MgCl_2$, and 2.0 $CaCl_2$. After equilibration with 95% O_2–5% CO_2, pH was adjusted to 7.35 if needed by NaOH or HCl. The intracellular pipette solution contained (in mM): 130 K gluconate, 1 $MgCl_2$, 10 HEPES, 0.3 EGTA, 10 Tris-Phosphocreatine, 4 Mg-ATP, 0.3 Na-GTP. When testing the contribution of BK channels, 300 nM Iberiotoxin (Abcam, Cambridge, United Kingdom) was included in the bath solution.

Conditions III and IV

The extracellular bath solution contained (in mM): 125 NaCl, 3 KCl, 25 Glucose, 25 $NaHCO_3$, 1.25 Na_2HPO_4, 1.1 $MgCl_2$, and 1.1 $CaCl_2$. After equilibration with 95% O_2–5% CO_2, pH was adjusted to 7.35 if needed by NaOH or HCl. The intracellular pipette solution contained (in mM): 150 K Gluconate, 10 K-HEPES, 3 Mg-ATP, 0.3 Na-GTP, 0.05 EGTA, 10 NaCl.

Conditions V and VI

The extracellular bath solution contained (in mM): 150 NaCl, 4 KCl, 10 HEPES, 10 glucose, 1.0 $MgCl_2$, and 2.0 $CaCl_2$, and was equilibrated with 95% O_2–5% CO_2. The intracellular pipette solution contained (in mM): 135 K gluconate, 4 NaCl, 0.05 EGTA, 10 HEPES, 3 $MgCl_2$, 0.3 NaGTP, 3 Na_2ATP, 10 Na_2-Creatine phosphate with pH normalized to 7.25 using KOH.

Condition VIII

The extracellular bath solution contained (in mM): 122 NaCl, 3 KCl, 1.25 NaH_2PO_4, 26 $NaHCO_3$, 10 glucose, 1.3 $MgCl_2$, and 2.0 $CaCl_2$, and was bubbled with 95% O_2–5% CO_2. The intracellular pipette solution contained (in mM): 130 K gluconate, 0.3 EGTA, 10 HEPES, 2 $MgCl_2$, 0.3 NaGTP, 4 Na_2ATP (or Mg-ATP), 10 Na_2-Creatine phosphate (or Tris-Creatinine phosphate).

Conditions IX and X

The extracellular bath solution contained (in mM): 145 NaCl, 2.5 KCl, 10 HEPES, 24 glucose, 1.3 $MgCl_2$, and 2.0 $CaCl_2$, and was equilibrated with 95% O_2–5% CO_2. The intracellular pipette solution contained (in mM): 140 K gluconate, 2 NaCl, 0.5 EGTA, 20 HEPES, 3 $MgCl_2$, 0.3 NaGTP, 4 Na_2ATP, with pH adjusted to 7.25 using KOH.

Organotypic hippocampal neuron recordings

The external bath solution contained (in mM): 125 NaCl, 26 $NaHCO_3$, 3 $CaCl_2$, 2.5 KCl, 2 $MgCl_2$, 0.8 NaH_2PO_4, and 10 D-glucose, and was equilibrated with 95% O_2–5% CO_2. The intracellular pipette solution contained (mM): 120 K gluconate, 20 KCl, 10 HEPES, 0.5 EGTA, 2 $MgCl_2$, 2 Na_2ATP, and 0.3 NaGTP (pH 7.4).

Statistics

If not otherwise noted, data are expressed as box plots with boxes reflecting 25^{th}–75^{th} percentile. The median is indicated by a line within the box, whiskers indicate 10^{th} and 90^{th} percentile. Sample sizes (n) provide the number of individual somatic recordings. All data sets were obtained from ≥ 2 independent cell cultures. Data in Fig. 3A were tested for statistical difference using Fisher's exact test. Confidence limits for 95% confidence intervals were calculated as Wilson interval[87]. Other experimental groups were independent and tested by the Mann-Whitney *U* test. Tests were performed in IGOR PRO or GraphPad Prism 8. Results were considered significant at $p < 0.05$.

Figure supplements

Group	Species	Strain	Brain area	Culture age (days *in vitro*)	Lab which recordings were performed at	External recording solution	External [Ca^{2+}] (mM)	Internal recording solution	Growth medium	Protocol Reference
I	Rat	Sprague-Dawley	Cortex	10–14	Hallermann Lab, Leipzig (Germany)	1.)	2.0	5.)	NbActiv4	Li *et al.*, Cell 2020
II	Rat	Sprague-Dawley	Cortex	16–21	Hallermann Lab, Leipzig (Germany)	1.)	2.0	5.)	NbActiv4	Li *et al.*, Cell 2020
III	Mouse	C57BL/6N	Cortex	15–20	Hallermann Lab, Leipzig (Germany)	2.)	1.1	6.)	BrainPhys	Moutin *et al.*, Front. Synaptic Neurosci 2020
IV	Mouse	C57BL/6N	Cortex	16	Hallermann Lab, Leipzig (Germany)	2.)	1.1	6.)	MEM, 5% serum + supplements	Ritzau-Jost *et al.*, Cell Reports 2021
V	Mouse	C57BL/6J	Cortex	11–13	Smith Lab, Portland (OR, USA)	3.)	2.0	7.)	MEM, 5% serum + supplements	Martiszus BJ *et al.*, eLife 2021
VI	Mouse	CD1	Cortex	11–13	Smith Lab, Portland (OR, USA)	3.)	2.0	7.)	MEM, 5% serum + supplements	Martiszus BJ *et al.*, eLife 2021
VII	Rat	Sprague-Dawley	Pre-frontal cortex	10–14	Hallermann Lab, Leipzig (Germany)	1.)	2.0	5.)	BrainPhys	Moutin *et al.*, Front. Synaptic Neurosci 2020
VIII	Mouse	C57BL/6J	Pre-frontal cortex	10–14	Smith Lab, Portland (OR, USA)	1.)	2.0	8.)	MEM, 5% serum + supplements	Martiszus BJ *et al.*, eLife 2021
IX	Mouse	C57BL/6N	Hippo-campus	32	Heine Lab, Mainz (Germany)	4.)	2.0	9.)	Neurobasal A+ supplements	Li *et al.*, Cell 2020
X	Mouse	C57BL/6J	Hippo-campus	15	Heine Lab, Mainz (Germany)	4.)	2.0	9.)	Neurobasal A + supplements	Li *et al.*, Cell 2020
XI	Rat	Sprague-Dawley	Hippo-campus	16–20	Hallermann Lab, Leipzig (Germany)	1.)	2.0	5.)	BrainPhys	Moutin *et al.*, Front. Synaptic Neurosci 2020

1.) 122 NaCl, 3 KCl, 10 Glucose, 26 $NaHCO_3$, 2 $CaCl_2$, 1.3 $MgCl_2$, 1.25 NaH_2PO_4
2.) 125 NaCl, 3 KCl, 25 Glucose, 25 $NaHCO_3$, 1.1 $CaCl_2$, 1.1 $MgCl_2$, 1.25 Na_2HPO_4
3.) 150 NaCl, 4 KCl, 10 Glucose, 10 HEPES, 2 $CaCl_2$, 1 $MgCl_2$
4.) 145 NaCl, 2.5 KCl, 24 Glucose, 10 HEPES, 2 $CaCl_2$, 1.3 $MgCl_2$
5.) 130 K gluconate, 10 HEPES, 1 $MgCl_2$, 0.3 EGTA, 4 Mg-ATP, 0.3 Na-GTP, 10 Tris-Phosphocreatine
6.) 150 K gluconate, 10 K-HEPES, 10 NaCl, 0.05 EGTA, 3 Mg-ATP, 0.3 Na-GTP
7.) 135 K gluconate, 10 HEPES, 4 NaCl, 0.05 EGTA, 3 Na_2ATP, 0.3 NaGTP, 3 $MgCl_2$, 10 Na_2-Creatine phosphate
8.) 130 K gluconate, 10 HEPES, 0.3 EGTA, 4 Na_2ATP (or Mg-ATP), 0.3 NaGTP, 2 $MgCl_2$, 10 Na_2-Creatine phosphate (or Tris-Creatinine phosphate)
9.) 140 K gluconate, 20 HEPES, 2 NaCl, 0.5 EGTA, 4 Na_2ATP, 0.3 NaGTP, 3 $MgCl_2$

Figure 2 – figure supplement 1. Additional information on recording conditions The table lists additional relevant information on the experimental conditions I – XI.

Figure 2 – figure supplement 2. Absence of TTX-induced AP broadening in further selected conditions

(A) Box plots of AP durations under control condition (black) or upon TTX-treatment (blue) recorded in condition I either unselected or selected for parameters reflecting unimpaired neuronal function. (B) AP durations as in A for recordings in condition VII. (C) AP durations as in A for recordings in condition VIII. Numbers of recorded neurons provided in brackets. Box plots depict median ± interquartile range, whiskers reflect 10–90 percentile. P-values calculated by Mann-Whitney-*U* test.

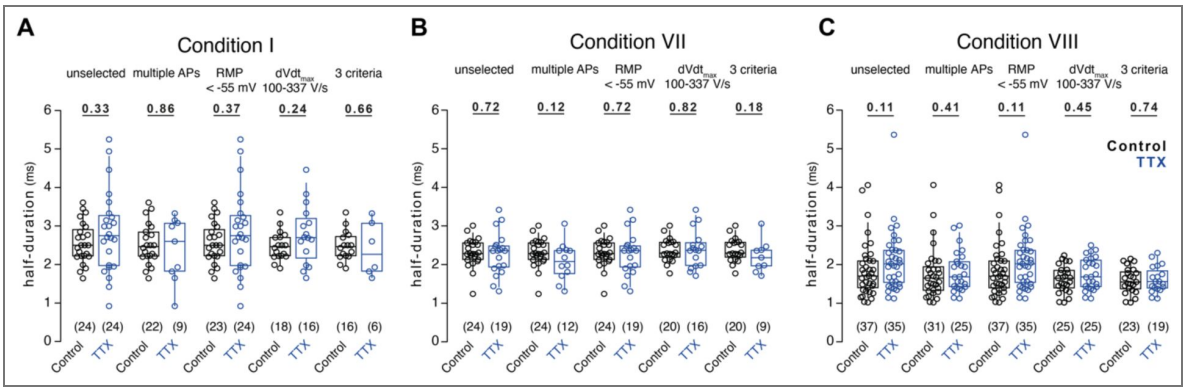

Figure 4 – figure supplement 1. BK channel block does not affect rebound AP duration

(A) Example rebound APs in control solution (black) and solution containing 300 nM Iberiotoxin (IbTx, green). (B) AP duration in control and TTX-treated cells in IbTx-free (black and blue, respectively) or IbTx-containing solution (green). Data recorded in condition I. (C) Merged AP duration across control and TTX-treated cells for recordings in IbTx-free and IbTx-containing solution (data in A, normalized to the respective group's median duration in IbTx-free solution). Numbers of recorded neurons provided in brackets. Box plots depict median ± interquartile range, whiskers reflect 10–90 percentile. P-values calculated by Mann-Whitney-*U* test.

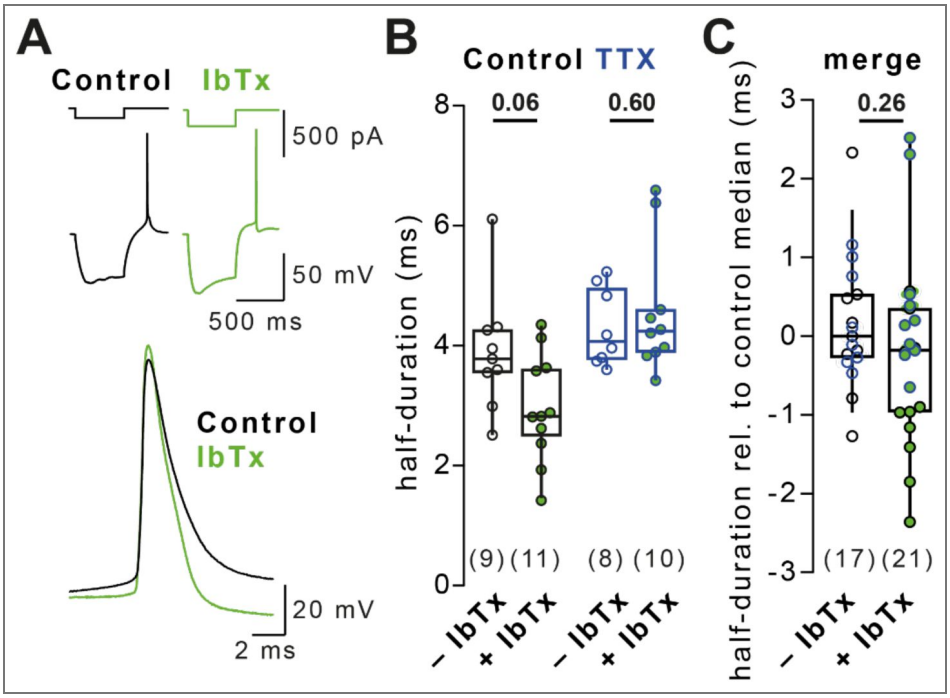

Data availability

All data generated in this study will be made available upon reasonable request to any of the corresponding authors.

Acknowledgements

This work was supported by a European Research Council Consolidator Grant (ERC CoG 865634) the German Research Foundation (HA6386/10-2) to S.H. and by grants awarded by the U.S. Department of Veterans Affairs (BX002547) and NIGMS (GM134110) to S.M.S.

Additional information

Funding

Funder	Grant reference number	Author
EC | European Research Council (ERC)	https://doi.org/10.3030/865634	Stefan Hallermann
Deutsche Forschungsgemeinschaft (DFG)	HA6386/10-2	Stefan Hallermann
U.S. Department of Veterans Affairs (VA)	BX002547	Stephen M Smith
HHS | NIH | National Institute of General Medical Sciences (NIGMS)	GM134110	Stephen M Smith

Author ORCID iDs

Andreas Ritzau-Jost: https://orcid.org/0000-0002-3922-949X
Jana Nerlich: https://orcid.org/0000-0002-6450-6380
Maren Engelhardt: https://orcid.org/0000-0001-8020-6604
Juan Burrone: https://orcid.org/0000-0003-1233-668X
Dominique Debanne: https://orcid.org/0000-0001-8581-5695
Stephen M Smith: https://orcid.org/0000-0002-0331-7615
Stefan Hallermann: https://orcid.org/0000-0001-9376-7048

References

1. **Borst J.G.G.,** Sakmann B (1999) Effect of changes in action potential shape on calcium currents and transmitter release in a calyx-type synapse of the rat auditory brainstem. *Philosophical Transactions of the Royal Society B: Biological Sciences* **354**:347-355 https://doi.org/10.1098/RSTB.1999.0386 | PubMed
2. **Christie B.R.,** Eliot L.S., Ito K.I., Miyakawa H., Johnston D (1995) Different Ca2+ channels in soma and dendrites of hippocampal pyramidal neurons mediate spike-induced Ca2+ influx. *J. Neurophysiol* **73**:2553-2557 https://doi.org/10.1152/jn.1995.73.6.2553 | PubMed
3. **Watanabe S.,** Hoffman D.A., Migliore M., Johnston D (2002) Dendritic K+ channels contribute to spike-timing dependent long-term potentiation in hippocampal pyramidal neurons. *Proc. Natl. Acad. Sci. U. S. A* **99**:8366-8371 https://doi.org/10.1073/PNAS.122210599 | PubMed
4. **Bean B.P** (2007) The action potential in mammalian central neurons. *Nat. Rev. Neurosci* **8**:451-465 https://doi.org/10.1038/nrn2148 | PubMed
5. **Debanne D.,** Campanac E., Bialowas A., Carlier E., Alcaraz G (2011) Axon physiology. *Physiol. Rev* **91**:555-602 https://doi.org/10.1152/PHYSREV.00048.2009 | PubMed
6. **Geiger J.R.P.,** Jonas P (2000) Dynamic control of presynaptic Ca2+ inflow by fast-inactivating K+ channels in hippocampal mossy fiber boutons. *Neuron* **28**:927-939 https://doi.org/10.1016/S0896-6273(00)00164-1 | PubMed

7. **Jackson M.B.,** Konnerth A., Augustine G.J (1991) Action potential broadening and frequency-dependent facilitation of calcium signals in pituitary nerve terminals. *Proc. Natl. Acad. Sci. U. S. A* **88**:380-384 https://doi.org/10.1073/PNAS.88.2.380 | PubMed

8. **Keck T.,** Toyoizumi T., Chen L., Doiron B., Feldman D.E., Fox K., Gerstner W., Haydon P.G., Hübener M., Lee H.K., *et al.* (2017) Integrating Hebbian and homeostatic plasticity: The current state of the field and future research directions. *Philosophical Transactions of the Royal Society B: Biological Sciences* **372** https://doi.org/10.1098/rstb.2016.0158 | PubMed

9. **Carta M.,** Lanore F., Rebola N., Szabo Z., Da Silva S.V., Lourenço J., Verraes A., Nadler A., Schultz C., Blanchet C., *et al.* (2014) Membrane lipids tune synaptic transmission by direct modulation of presynaptic potassium channels. *Neuron* **81**:787-799 https://doi.org/10.1016/J.NEURON.2013.12.028 | PubMed

10. **Senn V.,** Wolff S.B.E., Herry C., Grenier F.O., Ehrlich I., Grü J., Fadok J.P., Müller C., Letzkus J.J., Lüthi A (2014) Long-range connectivity defines behavioral specificity of amygdala neurons. *Neuron* **81**:428-437 https://doi.org/10.1016/j.neuron.2013.11.006 | PubMed

11. **Turrigiano G.G.,** Nelson S.B (2004) Homeostatic plasticity in the developing nervous system. *Nat. Rev. Neurosci* **5**:97-107 https://doi.org/10.1038/nrn1327 | PubMed

12. **Pozo K.,** Goda Y (2010) Unraveling mechanisms of homeostatic synaptic plasticity. *Neuron* **66**:337-351 https://doi.org/10.1016/J.NEURON.2010.04.028 | PubMed

13. **Li B.,** Suutari B.S., Sun S.D., Luo Z., Wei C., Chenouard N., Mandelberg N.J., Zhang G., Wamsley B., Tian G., *et al.* (2020) Neuronal inactivity co-opts LTP machinery to drive potassium channel splicing and homeostatic spike widening. *Cell* **181**:1547-1565.e15. https://doi.org/10.1016/j.cell.2020.05.013 | PubMed

14. **Ritzau-Jost A.,** Tsintsadze T., Krueger M., Ader J., Bechmann I., Eilers J., Barbour B., Smith S.M., Hallermann S (2021) Large, stable spikes exhibit differential broadening in excitatory and inhibitory neocortical boutons. *Cell Rep* **34**:108612 https://doi.org/10.1016/j.celrep.2020.108612 | PubMed

15. **Zbili M.,** Rama S., Benitez M.J., Fronzaroli-Molinieres L., Bialowas A., Boumedine-Guignon N., Garrido J.J., Debanne D (2021) Homeostatic regulation of axonal Kv1.1 channels accounts for both synaptic and intrinsic modifications in the hippocampal CA3 circuit. *Proc. Natl. Acad. Sci. U. S. A* **118** https://doi.org/10.1073/pnas.2110601118 | PubMed

16. **Kim J.,** Tsien R.W (2008) Synapse-specific adaptations to inactivity in hippocampal circuits achieve homeostatic gain control while dampening network reverberation. *Neuron* **58**:925-937 https://doi.org/10.1016/j.neuron.2008.05.009 | PubMed

17. **Mitra A.,** Mitra S.S., Tsien R.W (2012) Heterogeneous reallocation of presynaptic efficacy in recurrent excitatory circuits adapting to inactivity. *Nat. Neurosci* **15**:250-257 https://doi.org/10.1038/nn.3004 | PubMed

18. **Castro-Alamancos M.A.,** Connors B.W (1997) Distinct forms of short-term plasticity at excitatory synapses of hippocampus and neocortex. *Proc. Natl. Acad. Sci. U. S. A* **94**:4161-4166 https://doi.org/10.1073/pnas.94.8.4161 | PubMed

19. **Manahan-Vaughan D** (2018) Special considerations when using mice for In vivo electrophysiology and long-term studies of hippocampal synaptic plasticity during behavior. Handb. *Behav. Neurosci* **28**:63-84 https://doi.org/10.1016/B978-0-12-812028-6.00003-3

20. **Nguyen P. V.,** Duffy S.N., Young J.Z (2000) Differential maintenance and frequency-dependent tuning of LTP at hippocampal synapses of specific strains of inbred mice. *J. Neurophysiol* **84**:2484-2493 https://doi.org/10.1152/jn.2000.84.5.2484 | PubMed

21. **Prestigio C.,** Ferrante D., Valente P., Casagrande S., Albanesi E., Yanagawa Y., Benfenati F., Baldelli P (2019) Spike-Related Electrophysiological Identification of Cultured Hippocampal Excitatory and Inhibitory Neurons. *Mol. Neurobiol* **56**:6276-6292 https://doi.org/10.1007/s12035-019-1506-5 | PubMed

22. **Maffei A.,** Turrigiano G.G (2008) Multiple modes of network homeostasis in visual cortical layer 2/3. *Journal of Neuroscience* **28**:4377-4384 https://doi.org/10.1523/JNEUROSCI.5298-07.2008 | PubMed

23. **Desai N.S.,** Rutherford L.C., Turrigiano G.G (1999) Plasticity in the intrinsic excitability of cortical pyramidal neurons. *Nat. Neurosci* **2**:515-520 https://doi.org/10.1038/9165 | PubMed

24. **Turrigiano G.G.,** Leslie K.R., Desai N.S., Rutherford L.C., Nelson S.B (1998) Activity-dependent scaling of quantal amplitude in neocortical neurons. *Nature* **391**:892-896 https://doi.org/10.1038/36103 | PubMed

25. **Hanes A.L.,** Koesters A.G., Fong M.-F., Altimimi H.F., Stellwagen D., Wenner P., Engisch K.L (2020) Cellular/molecular divergent synaptic scaling of miniature EPSCs following activity blockade in dissociated neuronal cultures. *The Journal of neuroscience : the official journal of the Society for Neuroscience* **40**:4090-4102 https://doi.org/10.1523/JNEUROSCI.1393-19.2020 | PubMed

26. **Frank C.A.,** Kennedy M.J., Goold C.P.P., Marek K.W., Davis G.W.W (2006) Mechanisms underlying the rapid induction and sustained expression of synaptic homeostasis. *Neuron* **52**:663-677 https://doi.org/10.1016/J.NEURON.2006.09.029 | PubMed

27. **Aoto J.,** Nam C.I., Poon M.M., Ting P., Chen L (2008) Synaptic Signaling by All-Trans Retinoic Acid in Homeostatic Synaptic Plasticity. *Neuron* **60**:308-320 https://doi.org/10.1016/j.neuron.2008.08.012 | PubMed

28. **Gonzalez Sabater V.,** Rigby M., Burrone J. (2021) Voltage-gated potassium channels ensure action potential shape fidelity in distal axons. *The Journal of Neuroscience* **41**:5372-5385 https://doi.org/10.1523/jneurosci.2765-20.2021

29. **Hu H.,** Shao L.-R., Chavoshy S., Gu N., Trieb M., Behrens R., Laake P., Pongs O., Knaus H.G., Ottersen O.P., *et al.* (2001) Presynaptic Ca2+-activated K+ channels in glutamatergic hippocampal terminals and their role in spike repolarization and regulation of transmitter release. *The Journal of Neuroscience* **21**:9585-9597 https://doi.org/10.1523/JNEUROSCI.21-24-09585.2001 | PubMed

30. **Lorenzo-Ceballos Y.,** Carrasquel-Ursulaez W., Castillo K., Alvarez O., Latorre R (2019) Calcium-driven regulation of voltagesensingdomains in BK channels. *eLife* **8**:1-24 https://doi.org/10.7554/eLife.44934 | PubMed

31. **Karmarkar U.R.,** Buonomano D. V (2006) Different forms of homeostatic plasticity are engaged with distinct temporal profiles. *European Journal of Neuroscience* **23**:1575-1584 https://doi.org/10.1111/j.1460-9568.2006.04692.x | PubMed

32. **Horrigan F.T.,** Aldrich R.W (2002) Coupling between voltage sensor activation, Ca2+ binding and channel opening in large conductance (BK) potassium channels. *Journal of General Physiology* **120**:267-305 https://doi.org/10.1085/jgp.20028605 | PubMed

33. **Lee K.Y.,** Chung H.J (2014) NMDA receptors and L-type voltage-gated Ca2+ channels mediate the expression of bidirectional homeostatic intrinsic plasticity in cultured hippocampal neurons. *Neuroscience* **277**:610-623 https://doi.org/10.1016/j.neuroscience.2014.07.038 | PubMed

34. **Lee K.Y.,** Royston S.E., Vest M.O., Ley D.J., Lee S., Bolton E.C., Chung H.J (2015) N-methyl-D-aspartate receptors mediate activity-dependent down-regulation of potassium channel genes during the expression of homeostatic intrinsic plasticity. *Mol. Brain* **8**:1-16 https://doi.org/10.1186/s13041-015-0094-1 | PubMed

35. **Zhao C.J.,** Dreosti E., Lagnado L (2011) Homeostatic synaptic plasticity through changes in presynaptic calcium influx. *Journal of Neuroscience* **31**:7492-7496 https://doi.org/10.1523/JNEUROSCI.6636-10.2011 | PubMed

36. **Desai N.S.,** Rutherford L.C., Turrigiano G.G (1999) BDNF regulates the intrinsic excitability of cortical neurons. *Learning and Memory* **6**:284-291 https://doi.org/10.1101/lm.6.3.284 | PubMed

37. **Rutherford L.C.,** DeWan A., Lauer H.M., Turrigiano G.G (1997) Brain-derived neurotrophic factor mediates the activity-dependent regulation of inhibition in neocortical cultures. *Journal of Neuroscience* **17**:4527-4535 https://doi.org/10.1523/jneurosci.17-12-04527.1997 | PubMed

38. **Ritzau-Jost A.,** Nerlich J., Kaas T., Krueger M., Tsintsadze T., Eilers J., Barbour B., Smith S.M., Hallermann S (2023) Direct whole-cell patch-clamp recordings from small boutons in rodent primary neocortical neuron cultures. *STAR Protoc* **4**:102168 https://doi.org/10.1016/j.xpro.2023.102168 | PubMed

39. **Ivenshitz M.,** Segal M (2010) Neuronal density determines network connectivity and spontaneous activity in cultured hippocampus. *J. Neurophysiol* **104**:1052-1060 https://doi.org/10.1152/jn.00914.2009 | PubMed

40. **Mattson M.P.,** Kater S.B (1989) Development and selective neurodegeneration in cell cultures from different hippocampal regions. *Brain Res* **490**:110-125 https://doi.org/10.1016/0006-8993(89)90436-8 | PubMed

41. **Chipman P.H.,** Fetter R.D., Panzera L.C., Bergerson S.J., Karmelic D., Yokoyama S., Hoppa M.B., Davis G.W (2022) NMDAR-dependent presynaptic homeostasis in adult hippocampus: Synapse growth and cross-modal inhibitory plasticity. *Neuron* **110** https://doi.org/10.1016/j.neuron.2022.08.014 | PubMed

42. **Vinet J.,** van Weering H.R.J., Heinrich A., Kälin R.E., Wegner A., Brouwer N., Heppner F.L., van Rooijen N., Boddeke H.W.G.M., Biber K. (2012) Neuroprotective function for ramified microglia in hippocampal excitotoxicity. *J. Neuroinflammation* **9**:1-15 https://doi.org/10.1186/1742-2094-9-27 | PubMed

43. **Niday Z.,** Bean B.P (2021) BK channel regulation of afterpotentials and burst firing in cerebellar purkinje neurons. *Journal of Neuroscience* **41**:2854-2869 https://doi.org/10.1523/JNEUROSCI.0192-20.2021 | PubMed

44. **Gittis A.H.,** Moghadam S.H., Du Lac S. (2010) Mechanisms of sustained high firing rates in two classes of vestibular nucleus neurons: Differential contributions of resurgent Na, Kv3, and BK currents. *J. Neurophysiol* **104**:1625-1634 https://doi.org/10.1152/jn.00378.2010 | PubMed

45. **Kimm T.,** Khaliq Z.M., Bean B.P (2015) Differential regulation of action potential shape and burst-frequency firing by BK and Kv2 channels in substantia nigra dopaminergic neurons. *Journal of Neuroscience* **35**:16404-16417 https://doi.org/10.1523/JNEUROSCI.5291-14.2015 | PubMed

46. **Müller A.,** Kukley M., Uebachs M., Beck H., Dietrich D (2007) Nanodomains of single Ca2+ channels contribute to action potential repolarization in cortical neurons. *Journal of Neuroscience* **27**:483-495 https://doi.org/10.1523/JNEUROSCI.3816-06.2007 | PubMed

47. **Bock T.,** Stuart G.J (2016) The impact of BK channels on cellular excitability depends on their subcellular location. *Front. Cell. Neurosci* **10**:1-8 https://doi.org/10.3389/fncel.2016.00206 | PubMed

48. **Desai N.S.,** Cudmore R.H., Nelson S.B., Turrigiano G.G (2002) Critical periods for experience-dependent synaptic scaling in visual cortex. *Nat. Neurosci* **5**:783-789 https://doi.org/10.1038/nn878 | PubMed

49. **Wiesel T.N.,** Hubel D.H (1963) Single-cell responses in striate cortex of kittens deprived of vision in one eye. *J. Neurophysiol* **26**:1003-1017 https://doi.org/10.1152/jn.1963.26.6.1003 | PubMed

50. **Wen W.,** Turrigiano G.G (2021) Developmental regulation of homeostatic plasticity in mouse primary visual cortex. *The Journal of Neuroscience* **41**:JN-RM-1200-21 https://doi.org/10.1523/jneurosci.1200-21.2021 | PubMed

51. **Trojanowski N.F.,** Turrigiano G.G (2021) CaMKIV signaling is not essential for the maintenance of intrinsic or synaptic properties in mouse visual cortex. *eNeuro* **8**:1-12 https://doi.org/10.1523/ENEURO.0135-21.2021 | PubMed

52. **Griffen T.C.,** Haley M.S., Fontanini A., Maffei A (2017) Rapid plasticity of visually evoked responses in rat monocular visual cortex. *PLoS One* **12**:1-12 https://doi.org/10.1371/journal.pone.0184618 | PubMed

53. **Gainey M.A.,** Aman J.W., Feldman D.E (2018) Rapid disinhibition by adjustment of PV intrinsic excitability during whisker map plasticity in mouse S1. *Journal of Neuroscience* **38**:4749-4761 https://doi.org/10.1523/JNEUROSCI.3628-17.2018 | PubMed

54. **Maravall M.,** Stern E.A., Svoboda K (2004) Development of intrinsic properties and excitability of layer 2/3 pyramidal neurons during a critical period for sensory maps in rat barrel cortex. *J. Neurophysiol* **92**:144-156 https://doi.org/10.1152/jn.00598.2003 | PubMed

55. **Breton J.D.,** Stuart G.J (2009) Loss of sensory input increases the intrinsic excitability of layer 5 pyramidal neurons in rat barrel cortex. *J. Physiol* **587**:5107-5119 https://doi.org/10.1113/JPHYSIOL.2009.180943 | PubMed

56. **Sun Q.Q** (2009) Experience-dependent intrinsic plasticity in interneurons of barrel cortex layer IV. *J. Neurophysiol* **102**:2955-2973 https://doi.org/10.1152/jn.00562.2009 | PubMed

57. **Li L.,** Gainey M.A., Goldbeck J.E., Feldman D.E (2014) Rapid homeostasis by disinhibition during whisker map plasticity. *Proc. Natl. Acad. Sci. U. S. A* **111**:1616-1621 https://doi.org/10.1073/pnas.1312455111 | PubMed

58. **Jamann N.,** Dannehl D., Lehmann N., Wagener R., Thielemann C., Schultz C., Staiger J., Kole M.H.P., Engelhardt M (2021) Sensory input drives rapid homeostatic scaling of the axon initial segment in mouse barrel cortex. *Nat. Commun* **12**:1-14 https://doi.org/10.1038/s41467-020-20232-x | PubMed

59. **Hickmott P.W** (2005) Changes in intrinsic properties of pyramidal neurons in adult rat S1 during cortical reorganization. *J. Neurophysiol* **94**:501-511 https://doi.org/10.1152/jn.00924.2004 | PubMed

60. **Francis H.W.,** Manis P.B (2000) Effects of deafferentation on the electrophysiology of ventral cochlear nucleus neurons. *Hear Res* **149**:91-105 https://doi.org/10.1016/S0378-5955(00)00165-9 | PubMed

61. **Lu Y.,** Monsivais P., Tempel B.L., Rubel E.W (2004) Activity-dependent regulation of the potassium channel subunits Kv1.1 and Kv3.1. *Journal of Comparative Neurology* **470**:93-106 https://doi.org/10.1002/cne.11037 | PubMed

62. **Wang Y.,** Manis P.B (2006) Temporal coding by cochlear nucleus bushy cells in DBA/2J mice with early onset hearing loss. *JARO - Journal of the Association for Research in Otolaryngology* **7**:412-424 https://doi.org/10.1007/s10162-006-0052-9 | PubMed

63. **Leao R.N.,** Berntson A., Forsythe I.D., Walmsley B (2004) Reduced low-voltage activated K+ conductances and enhanced central excitability in a congenitally deaf (dn/dn) mouse. *J. Physiol* **559**:25-33 https://doi.org/10.1113/JPHYSIOL.2004.067421 | PubMed

64. **Him A.,** Dutia M.B (2001) Intrinsic excitability changes in vestibular nucleus neurons after unilateral deafferentation. *Brain Res* **908**:58-66 https://doi.org/10.1016/S0006-8993(01)02600-2

65. **George N.M.,** Gentile Polese A., Merle L., Macklin W.B., Restrepo D (2022) Excitable axonal domains adapt to sensory deprivation in the olfactory system. *The Journal of Neuroscience* **42**:1491-1509 https://doi.org/10.1523/JNEUROSCI.0305-21.2021 | PubMed

66. **Barnes B.Y.C.A.,** McNaughton B.L (1980) Physiological compensation for loss of afferent synapses in rat hippocampal granule cells during senescence. *J. Physiol* **309**:473-485 https://doi.org/10.1113/jphysiol.1980.sp013521

67. **Midorikawa M.,** Miyata M (2021) Distinct functional developments of surviving and eliminated presynaptic terminals. *Proc. Natl. Acad. Sci. U. S. A* **118** https://doi.org/10.1073/pnas.2022423118 | PubMed

68. **O'Leary T.,** van Rossum M.C.W., Wyllie D.J.A. (2010) Homeostasis of intrinsic excitability in hippocampal neurones: Dynamics and mechanism of the response to chronic depolarization. *Journal of Physiology* **588**:157-170 https://doi.org/10.1113/jphysiol.2009.181024 | PubMed

69. **Pozzi D.,** Lignani G., Ferrea E., Contestabile A., Paonessa F., D'Alessandro R., Lippiello P., Boido D., Fassio A., Meldolesi J., *et al.* (2013) REST/NRSF-mediated intrinsic homeostasis protects neuronal networks from hyperexcitability. *EMBO Journal* **32**:2994-3007 https://doi.org/10.1038/emboj.2013.231 | PubMed

70. **Wefelmeyer W.,** Cattaert D., Burrone J (2015) Activity-dependent mismatch between axo-axonic synapses and the axon initial segment controls neuronal output. *Proc. Natl. Acad. Sci. U. S. A* **112**:9757-9762 https://doi.org/10.1073/pnas.1502902112 | PubMed

71. **Malik R.,** Chattarji S (2012) Enhanced intrinsic excitability and EPSP-spike coupling accompany enriched environment-induced facilitation of LTP in hippocampal CA1 pyramidal neurons. *J. Neurophysiol* **107**:1366-1378 https://doi.org/10.1152/jn.01009.2011 | PubMed

72. **Valero-Aracama M.J.,** Sauvage M.M., Yoshida M (2015) Environmental enrichment modulates intrinsic cellular excitability of hippocampal CA1 pyramidal cells in a housing duration and anatomical location-dependent manner. *Behavioural Brain Research* **292**:209-218 https://doi.org/10.1016/j.bbr.2015.05.032 | PubMed

73. **Kole M.H.P.,** Czéh B., Fuchs E (2004) Homeostatic maintenance in excitability of tree shrew hippocampal CA3 pyramidal neurons after chronic stress. *Hippocampus* **14**:742-751 https://doi.org/10.1002/hipo.10212 | PubMed

74. **Kamal A.,** Notenboom R.G.E., De Graan P.N.E., Ramakers G.M.J. (2006) Persistent changes in action potential broadening and the slow afterhyperpolarization in rat CA1 pyramidal cells after febrile seizures. *European Journal of Neuroscience* **23**:2230-2234 https://doi.org/10.1111/j.1460-9568.2006.04732.x | PubMed

75. **Eshra A.,** Hirrlinger P., Hallermann S (2019) Enriched environment shortens the duration of action potentials in cerebellar granule cells. *Front. Cell. Neurosci* **13**:1-9 https://doi.org/10.3389/fncel.2019.00289 | PubMed

76. **Ngodup T.,** Goetza J.A., McGuire B.C., Sun W., Lauer A.M., Xu-Friedman M.A (2015) Activity-dependent, homeostatic regulation of neurotransmitter release from auditory nerve fibers. *Proc. Natl. Acad. Sci. U. S. A* **112**:6479-6484 https://doi.org/10.1073/PNAS.1420885112

77. **Simkin D.,** Hattori S., Ybarra N., Musia T.F., Buss E.W., Richter H., Matthew Oh M., Nicholson D.A., Disterhoft J.F (2015) Aging-related hyperexcitability in CA3 pyramidal neurons is mediated by enhanced A-type K+ channel function and expression. *Journal of Neuroscience* **35**:13206-13218 https://doi.org/10.1523/JNEUROSCI.0193-15.2015 | PubMed

78. **Mehranfard N.,** Gholamipour-Badie H., Motamedi F., Janahmadi M., Naderi N (2015) Long-term increases in BK potassium channel underlie increased action potential firing in dentate granule neurons following pilocarpine-induced status epilepticus in rats. *Neurosci. Lett* **585**:88-91 https://doi.org/10.1016/j.neulet.2014.11.041 | PubMed

79. **Raffaelli G.,** Saviane C., Mohajerani M.H., Pedarzani P., Cherubini E (2004) BK potassium channels control transmitter release at CA3-CA3 synapses in the rat hippocampus. *Journal of Physiology* **557**:147-157 https://doi.org/10.1113/jphysiol.2004.062661 | PubMed

80. **Moutin E.,** Hemonnot A.L., Seube V., Linck N., Rassendren F., Perroy J., Compan V (2020) Procedures for culturing and genetically manipulating murine hippocampal postnatal neurons. *Front. Synaptic Neurosci* **12**:1-16 https://doi.org/10.3389/fnsyn.2020.00019 | PubMed

81. **Martiszus B.J.,** Tsintsadze T., Chang W., Smith S.M (2021) Enhanced excitability of cortical neurons in low-divalent solutions is primarily mediated by altered voltage-dependence of voltage-gated sodium channels. *eLife* **10**:1-26 https://doi.org/10.7554/eLife.67914 | PubMed

82. **Clements J.D.,** Bekkers J.M (1997) Detection of spontaneous synaptic events with an optimally scaled template. *Biophys. J* **73**:220-229 https://doi.org/10.1016/S0006-3495(97)78062-7 | PubMed

83. **Rothman J.S.,** Silver R.A (2018) Neuromatic: An integrated open-source software toolkit for acquisition, analysis and simulation of electrophysiological data. *Front. Neuroinform* **12**:1-21 https://doi.org/10.3389/fninf.2018.00014 | PubMed

84. **Debanne D.,** Boudkkazi S., Campanac E., Cudmore R.H., Giraud P., Fronzaroli-Molinieres L., Carlier E., Caillard O (2008) Paired-recordings from synaptically coupled cortical and hippocampal neurons in acute and cultured brain slices. *Nat. Protoc* **3**:1559-1568 https://doi.org/10.1038/nprot.2008.147 | PubMed

85. **Gong Y.,** Huang C., Li J.Z., Grewe B.F., Zhang Y., Eismann S., Schnitzer M.J (2015) High-speed recording of neural spikes in awake mice and flies with a fluorescent voltage sensor. *Science* **350**:1361-1366 https://doi.org/10.1126/science.aab0810 | PubMed

86. **Thevenaz P.,** Ruttimann U.E., Unser M (1998) A pyramid approach to subpixel registration based on intensity. *IEEE Transactions on Image Processing* **7**:27-41 https://doi.org/10.1109/83.650848 | PubMed

87. **Brown L.D.,** Cai T.T., DasGupta A (2001) Interval estimation for a binomial proportion. *Statistical Science* **16**:101-133 https://doi.org/10.1214/ss/1009213286

Peer reviews

Reviewer #1 (Public review):

[Editors' note: The Reviewing Editor has assessed the revised manuscript without seeking further input from the original reviewers. The authors have addressed the main points raised during peer review, including clarifying methodological differences with prior work, providing additional analysis, and expanding the discussion of potential mechanisms. These revisions strengthen the interpretation and presentation of the findings, and the conclusions remain supported by the data.]

Summary:

Ritzau-Jost et al. investigate the potential contribution of AP broadening in homeostatic upregulation of neuronal network activity with a specific focus on dissociated neuronal cultures. In cultures obtained from a few brain regions from mice or rats using different culture conditions and examined by different laboratories, AP half-width remained stable despite chronic activity block with TTX. The finding suggests that AP width is not significantly modulated by changes in sodium channel activity.

Strengths:

The collaborative nature of the study amongst the neuronal culture experts and the rigorous electrophysiological assessments provides for a compelling support of the main conclusion.

https://doi.org/10.7554/eLife.106995.2.sa3

Reviewer #2 (Public review):

Summary:

This study reexamined the idea that action potential broadening serves as a homeostatic mechanism to compensate for changes in network activity. The key finding was that, while action potential broadening does occur in certain neurons - such as CA3 pyramidal cells-it is far from a universal response. This is important because it helps resolve longstanding discrepancies in the field, thereby contributing to a better understanding of network dynamics. The replication of these findings across multiple laboratories further strengthened the study's rigor.

Strengths:

Mechanisms of network homeostasis are essential to understand network dynamics.

https://doi.org/10.7554/eLife.106995.2.sa2

Reviewer #3 (Public review):

Summary:

The manuscript "Unreliable homeostatic action potential broadening in cultured dissociated neurons" by Ritzau-Jost et al. investigates action potential (AP) broadening as a mechanism underlying homeostatic synaptic plasticity. Given the existing variability in the literature concerning AP broadening, the authors address an important and timely research question of considerable interest to the field.

The study systematically demonstrates cell-type- and model-specific AP broadening in hippocampal neurons after chronic treatment with either tetrodotoxin (TTX) or glutamatergic transmission blockers. The findings indicate AP broadening in CA3 pyramidal neurons in organotypic cultures after TTX treatment, but notably not in dissociated hippocampal neurons under identical conditions. However, blocking glutamatergic neurotransmission caused AP broadening in dissociated hippocampal neurons. Moreover, extensive evaluations in neocortical dissociated cultures robustly challenge previous findings by revealing a lack of AP broadening following TTX treatment. Additionally, the proposed role of BK-type potassium channels in mediating AP broadening is convincingly questioned through complementary electrophysiological and voltage-imaging experiments.

Strengths:

The manuscript exhibits an outstanding experimental design, employing state-of-the-art techniques and a rigorous multi-lab validation approach that greatly enhances scientific reliability. The experimental results are meticulously illustrated, and the conclusions drawn are justified and supported by the presented data. Furthermore, the manuscript is comprehensively and clearly written.

https://doi.org/10.7554/eLife.106995.2.sa1

Author response:

The following is the authors' response to the original reviews.

> ***Public Reviews:***
>
> ***Reviewer #1 (Public review):***
>
> *Summary:*
>
> *Ritzau-Jost et al. investigate the potential contribution of AP broadening in homeostatic upregulation of neuronal network activity with a specific focus on dissociated neuronal cultures. In cultures obtained from a few brain regions from mice or rats using different culture conditions and examined by different laboratories, AP half-width remained stable despite chronic activity block with TTX. The finding suggests that AP width is not significantly modulated by changes in sodium channel activity.*
>
> *Strengths:*
>
> *The collaborative nature of the study amongst the neuronal culture experts and the rigorous electrophysiological assessments provides for a compelling support of the main conclusion.*
>
> *Weaknesses:*
>
> *Given the negative nature of the results, a couple of remaining issues (such as the cell density of cultures and the presentation of imaging experiments with a voltage sensor) warrant further consideration. In addition, a discussion of the reasons for the I stability of AP half-width to sodium channel modulation might help extend the scope of the study beyond the presentation of a negative conclusion.*

We would like to thank the reviewer for positively evaluating our manuscript. Please find below our detailed point-to-point response to the reviewer's comments.

> ***Reviewer #2 (Public review):***
>
> *Summary:*

> *This study reexamined the idea that action potential broadening serves as a homeostatic mechanism to compensate for changes in network activity. The key finding was that, while action potential broadening does occur in certain neurons - such as CA3 pyramidal cells-it is far from a universal response. This is important because it helps resolve longstanding discrepancies in the field, thereby contributing to a better understanding of network dynamics. The replication of these findings across multiple laboratories further strengthened the study's rigor.*
>
> *Strengths:*
>
> *Mechanisms of network homeostasis are essential to understand network dynamics.*
>
> *Weaknesses:*
>
> *No weaknesses were noted by this reviewer.*

We would like to thank the reviewer for the positive evaluation of our manuscript. Please find below our detailed point-to-point response to the reviewer's comments.

> ***Reviewer #3 (Public review):***
>
> *Summary:*
>
> *The manuscript "Unreliable homeostatic action potential broadening in cultured dissociated neurons" by Ritzau-Jost et al. investigates action potential (AP) broadening as a mechanism underlying homeostatic synaptic plasticity. Given the existing variability in the literature concerning AP broadening, the authors address an important and timely research question of considerable interest to the field.*
>
> *The study systematically demonstrates cell-type- and model-specific AP broadening in hippocampal neurons after chronic treatment with either tetrodotoxin (TTX) or glutamatergic transmission blockers. The findings indicate AP broadening in CA3 pyramidal neurons in organotypic cultures after TTX treatment, but notably not in dissociated hippocampal neurons under identical conditions. However, blocking glutamatergic neurotransmission caused AP broadening in dissociated hippocampal neurons. Moreover, extensive evaluations in neocortical dissociated cultures robustly challenge previous findings by revealing a lack of AP broadening following TTX treatment. Additionally, the proposed role of BK-type potassium channels in mediating AP broadening is convincingly questioned through complementary electrophysiological and voltage-imaging experiments.*
>
> *Strengths:*
>
> *The manuscript exhibits an outstanding experimental design, employing state-of-the-art techniques and a rigorous multi-lab validation approach that greatly enhances scientific reliability. The experimental results are meticulously illustrated, and the conclusions drawn are justified and supported by the presented data. Furthermore, the manuscript is comprehensively and clearly written.*
>
> *Weaknesses:*
>
> *Concerning the statistical analyses employed, it is advisable to consider the Kruskal-Wallis test with corrections for multiple comparisons when evaluating more than two experimental groups.*

We would like to thank the reviewer for the positive evaluation of our manuscript. In the following we first address the comment regarding the used statistical tests. Please also find below the detailed response to the reviewer's further comments. Indeed, we did not apply a

correction for multiple comparisons in Figure 2. This seems justified because in this exceptional case we are more worried about type II errors (false negative). The Kruskal-Wallis test seems not appropriate for this type of data for which only the comparison between the control and respective TTX data is relevant. Instead, we followed the reviewer's suggestion by applying corrections for false discovery rate (FDR). We thank the reviewer for pointing out this statistical issue and addressed it in the revised manuscript (lines 121–128):

"Even though AP durations varied up to 2-fold between conditions, statistically significant homeostatic AP broadening was not detectable in any of the tested conditions (Fig. 2B). To minimize type II errors (false negative) we intentionally did not apply a correction for multiple comparisons. The only significance was observed in condition III but in an opposite direction (i.e. AP narrowing with TTX, P=0.026; Fig. 2B). However, this is likely a false positive because application of corrections for false discovery rate results in P=0.268 for both Benjamini–Hochberg and Bonferroni correction."

> ***Recommendations for the authors:***
>
> ***Reviewing Editor Comments:***
>
> *The main and most important observation of the study is that the AP does not change in most cases examined. A discussion of the mechanisms of the changes in CA3 neurons would significantly strengthen the compelling evidence presented. The individual reviews are also provided, in case the authors find them useful to include other aspects suggested by the reviewers.*

We would like to thank the Reviewing Editor for handing our manuscript and for the positive evaluation of our work. The main focus of our study was the analysis of homeostatic plasticity in cultured neurons of the neocortex. We agree that the findings in CA3 neurons are interesting. As explained in more detail below, we have carefully discussed the mechanisms of the changes in CA3 neurons in the revised manuscript.

> ***Reviewer #1 (Recommendations for the authors):***
>
> *Major points*
>
> *(1) AP widths measured in the present study under basal conditions are generally larger than the value reported in previous work by Li et al. 2020 (~1.5 ms). In particular, rat cortical cultures prepared using the same conditions show that the mean AP half-width in controls of the present study (~2.5 ms) is closer to the mean AP half-width in TTX-treated neurons in Li et al. (~2.0 ms).*

We thank the reviewer for the detailed and positive feedback as well as for the thoughtful questions. The inconsistency of action potential half-duration reported in our and Li et al.'s data is partially due to differences in the way the half-duration was measured. In Li et al. the exact method is unfortunately not defined, but from a personal communication with the authors we know that they measured half-duration based on the AP amplitude between AP peak and AP voltage threshold. In contrast, we measured half-duration based on the AP amplitude between AP peak and the resting membrane potential preceding current injections. When we measure AP half-duration instead from voltage threshold, the average half-durations are 1.97 ms (compared to 2.64 ms from baseline, n = 106 cells; average across conditions I–IV, control and TTX merged). Thus, the discrepancy in the half-duration is to a significant proportion due to methodical differences in the way the half-duration was measured.

> *One parameter that is not stated in either study is cell plating density, which can potentially bias the neuronal network activity levels of cultures. Could the authors comment on the possible contribution of neuronal culture density to AP half-width under*

> *basal recording conditions and its sensitivity to chronic TTX treatment? Are there any data available? For example, cultures used by Li et al may have been plated at a high density and experienced high activity level during culturing, which could have contributed to the enhanced sensitivity to chronic activity suppression by TTX.*

We agree that neuronal culture density is an important factor influencing neuronal activity and hence potentially also the sensitivity to chronic activity suppression. In our experiments, the number of plated cells per cover slip varied between conditions about 3-fold: 30–50k cells for conditions I and II, 25–30k cells for conditions III, VII, XI, 50k cells for condition IV, 65k for conditions V, VI and VIII, and 70k cells for conditions IX and X. Li et al. do not provide the cell density or the number of plated cells. Despite the difference in the number of plated cells in our dataset across various laboratories, we did not observe a systematic effect of cell number on baseline AP half-duration. Furthermore, we observed strongly different baseline activity across our various experimental conditions (Fig. 3A), which did not correlate with cell density. Also, we did not notice an impact of baseline activity on the sensitivity to chronic activity suppression with TTX (cf. Fig. 3A and 2B). We have now added the number of plated cells per condition to the methods section as well as the following paragraph to the discussion section (lines 256–262):

"The sensitivity to chronic TTX treatment might depend on baseline neuronal activity, which is in part related to neuronal culture density[37]. However, TTX did not induce AP broadening despite different baseline activities (Fig. 3A) and a nearly threefold variation in the number of plated cells per cover slip between conditions (25k – 70k cells per coverslip)."

> *In addition, a discussion of the reasons for the seeming stability of AP half-width to sodium channel modulation might help extend the scope of the study beyond the presentation of a negative conclusion.*

We thank the reviewer for this suggestion and have added a paragraph to the end of the discussion emphasizing potential advantages of cell-type specific AP broadening (lines 353–362):

"Despite the lack of homeostatic, TTX-induced AP broadening in dissociated cultures, AP duration was broadened upon Kyn-treatment in dissociated cultures and using TTX in CA3 neurons in organotypic cultures. Because BK-channels control AP duration in CA3 neurons of organotypic cultures[79], homeostatic BK-channel downregulation as proposed by Li et al. may be involved in AP broadening in this specific cell type. While the reasons for the variable occurrence of homeostatic AP broadening remain unknown, this may render neuronal circuitries more robust to perturbations. The regulation of AP duration therefore might represent one element in the repertoire of neuronal plasticity that is, similar to other plasticity mechanisms, not generally shared, but specifically expressed in some cell types and neuronal compartments."

> *(2) In this study, CA3 neurons in organotypic cultures were the only cells that showed AP broadening with TTX treatment. Notably, CA3 neurons show strong recurrent activity in general and would be expected to have experienced high levels of activity in culture. For CA3 neurons in organotypic cultures, does IbTx increase basal AP half-width?*

We thank the reviewer for this interesting idea. Even though, to our knowledge, there is no study investigating the effect of IbTx on AP width in CA3 neurons of organotypic cultures, Raffaelli et al. (DOI 10.1113/jphysiol.2004.062661) reported ~15% AP broadening using the BK-channel blocker paxilline. Therefore, TTX-induced broadening in CA3 neurons might be related to BK-channel-dependent AP repolarisation, consistent with the model proposed by Li et al. Because organotypic cultures show increased activity for longer cultivation periods and higher connectivity compared to acute slices (De Simoni et al., DOI 10.1113/jphysiol.2003.039099), the effect of TTX may be aggravated in organotypic cultures

compared to acute slices or in vivo. However, the lack of a TTX-effect was not dependent on background neuronal activity or culture density in our recordings (see above as well as lines 306–310 of the revised manuscript).

> *(3) Figures 4E-G. In experiments to test the efficacy of IbTx with GEVI, larger fields of view of neuron(s) used for recordings should be included. As shown, it is difficult to discern the quality of the preparation and does not provide a representative indication of the type of signals measured.*

We thank the reviewer for this suggestion and have included an image of a representative neuron expressing the GEVI in Fig. 4E.

> *Minor points*
>
> *(1) Lines 222-228. With respect to cell-type specificity of TTX-induced AP broadening, the observed lack of effect of TTX in dissociated hippocampal cultures might suggest that the cultures are predominantly DG granule cells and CA1 neurons, with few CA3 neurons surviving. Could the authors comment?*

We thank the review for this interesting hypothesis and have discussed it in the manuscript as a potential explanation for our different findings in the hippocampus.(lines 263–270):

“Although we mainly focus on neocortical cultured neurons (condition I to VIII, Fig. 2) because Li et al. used neocortical neurons, the absence of AP broadening in hippocampal neurons (group IX to XI) could in principle be explained by the selective loss of CA3 neurons, which show AP broadening in organotypic cultured neurons (Fig. 1A and B). However, CA3 neurons were shown to survive in dissociated cultures following region-specific microdissection[40], and CA1 neurons are generally more stress-sensitive to excitotoxicity with glutamate or NMDA than CA3 and DG neurons[42], arguing against a general selective loss of CA3 neuron in dissociated cultures.”

> *(2) Figures 3D, E. To what extent is the observed increase in sEPSC amplitude due to an increase in sEPSC frequency? Is quantal amplitude increased following TTX treatment, a postsynaptic strength parameter that one would not expect to be affected by a change in AP width, but that is known to undergo up-scaling with chronic TTX treatment?*

We would like to thank the reviewer for the question. We cannot rule out an interplay between sEPSC amplitude and frequency. We did not measure quantal amplitude in the presence of TTX. Our experiments were designed to test whether TTX successfully induced homeostatic plasticity, but not to attribute the observed effect to pre- and postsynaptic mechanisms. We have added the following statement to the revised manuscript, to highlight the possible interaction of sEPSC amplitude and frequency (lines 176–178):

“These changes in sEPSC amplitude and frequency are not specific for somatic, pre- or postsynaptic adaptations. However, the results show that blocking AP firing with TTX successfully induced homeostatic plasticity under our experimental conditions.”

> *(3) Line 132. Could the authors explain the rationale for using AP amplitude as a measure of neuronal "viability"?*

In a response to Cell, Li et al. suggested that the lack of a TTX effect was due to recordings from unhealthy neurons and that small AP amplitudes could indicate impaired cell viability. Indeed, we also believe that cells which appear morphologically less healthy tend to have small and slow APs. A mechanistic rationale could be a change resting membrane potential or changes in the expression of voltage-gated sodium and potassium channels. However, AP amplitudes were not affected following TTX treatment in any of the eleven recording

conditions (Fig. 2D) or a cross-conditional comparison (Fig. 2E). In the revised manuscript, we have now added a possible rationale (lines 134–137):

"Because unhealthy neurons tend to have small and slow APs, possibly due to changes in resting membrane potential or expression of voltage-gated sodium and potassium channels, we first analyzed AP amplitude as a measure of neuronal viability."

> ***Reviewer #3 (Recommendations for the authors):***
>
> *I propose addressing the following questions, either through additional experiments (recommended) or a deeper theoretical discussion:*
>
> *(1) Since the authors demonstrate that blocking glutamatergic neurotransmission in dissociated hippocampal neurons causes AP broadening, do similar phenomena occur in organotypic cultures and dissociated neocortical neurons?*

We thank the reviewer for the interesting question. In dissociated hippocampal cultures, we show that AP duration is maintained following treatment with TTX and NBXQ, while Kyn-treatment leads to AP broadening (Figure 1C). To our knowledge, the effect of Kyn on AP duration has not been studied in neocortical dissociated cultured neurons. However, Kyn induced AP broadening in CA3 neurons of hippocampal organotypic cultures (Zbili et al., DOI 10.1073/pnas.2110601118) while CNQX did not induce such broadening in CA1 neurons (Karmarkar and Buonomano, DOI 10.1111/j.1460-9568.2006.04692.x). Both findings are in accord with our recordings from dissociated hippocampal cultures. These data however do not allow inference as to whether AP broadening is a cell-type specific or blocker-specific mechanism in hippocampal organotypic cultures. Because the main focus of our study is the absence of AP broadening in neocortical cultured neurons as described by Li et al., we adjusted the corresponding discussion section (lines 299–322)

"In contrast, APs were not significantly broader following synaptic block by NBQX (Fig. 1C, D), in accord with recordings from CA1 neurons in organotypic cultures using CNQX. TTX-induced broadening may therefore be cell-type specific or due to a differential effect of the glutamate receptor blockers on NMDA receptors which are blocked by Kyn but not NBQX/CNQX or TTX and which have recently been demonstrated to be important for the induction of synaptic homeostatic plasticity[41]."

> *(2) Are BK channels involved in AP broadening observed in CA3 pyramidal neurons in organotypic cultures?*

We thank the reviewer for the question. BK channels control spike duration in CA3 neurons of organotypic cultures (~15% broadening upon block by paxilline; Raffaelli et al., DOI 10.1113/jphysiol.2004.062661). Even though there is no available data on the contribution of BK channels to homeostatic spike broadening in this cell type, CA3 neurons in organotypic cultures thereby fulfil the two necessary preconditions of the model proposed by Li et al. (namely, the control of the resting AP width by BK-channels and TTX-induced AP broadening). We include this possibility in the discussion (lines 355–357):

"Because BK-channels control AP duration in CA3 neurons of organotypic cultures[79], homeostatic BK-channel downregulation as proposed by Li et al. may be involved in AP broadening in this specific cell type."

> *(3) AP broadening consistently occurs in CA3 neurons within organotypic cultures; what molecular or cellular mechanisms underpin this phenomenon, and is there a potential contribution from glial cells?*

We thank the reviewer for this interesting question. CA3 neurons show AP broadening upon chronic inactivity across various studies that has not been observed in CA1 or DG neurons.

Recordings from CA3 neurons served as a positive example for TTX-induced AP broadening in our study, in contrast to a lack of broadening in dissociated (neocortical and hippocampal) cultured neurons. The discrepancy between the results in dissociated and organotypic cultured neurons could indeed be due to interactions with glia cells. We have added this possibility to the discussion in the revised version of the manuscript (lines 270–273)

“Altered cell-cell interactions with glia and neurons in organotypic and dissociated neuronal cultures could instead contribute to the different findings in various hippocampal preparations.”

https://doi.org/10.7554/eLife.106995.2.sa0